Flipped Classroom: Effective Teaching for Time Series Forecasting

Anonymous authors
Paper under double-blind review

Abstract

Sequence-to-sequence models based on LSTM and GRU are a most popular choice for forecasting time series data reaching state of the art performance. Training such models can be delicate though. The two most common training strategies within this context are teacher forcing (TF) and free running (FR). TF can be used to help the model to converge faster but may provoke an exposure bias issue due to a discrepancy between training and inference phase. FR helps to avoid this but does not necessarily lead to better results, since it tends to make the training slow and unstable instead. Scheduled sampling was the first approach tackling these issues by picking the best from both worlds and combining it into a curriculum learning (CL) strategy. Although scheduled sampling seems to be a convincing alternative to FR and TF, we found that, even if parametrized carefully, scheduled sampling may lead to premature termination of the training when applied for time series forecasting. To mitigate the problems of the above approaches we formalize CL strategies along the training as well as the training iteration scale. We propose several new curricula, and systematically evaluate their performance in two experimental sets. For our experiments, we utilize six datasets generated from prominent chaotic systems. We found that the newly proposed increasing training scale curricula with a probabilistic iteration scale curriculum consistently outperforms previous training strategies yielding an NRMSE improvement of up to 81% over FR or TF training. For some datasets we additionally observe a reduced number of training iterations. We observed that all models trained with the new curricula yield higher prediction stability allowing for longer prediction horizons.

1 Introduction

[1] Advanced Recurrent Neural Networks (RNNs) such as Long Short Term Memory (LSTM) (Hochreiter & Schmidhuber, 1997) and Gated Recurrent Unit (GRU) (Cho et al., 2014) achieved significant results in predicting sequential data (Chung et al., 2014; Nowak et al., 2017; Yin et al., 2017). Such sequential data can for example be textual data as processed for Natural Language Processing (NLP) tasks where RNN models were the method of choice for a long time, before feed-forward architectures like transformers showed superior results in processing natural language data (Devlin et al., 2018; Yang et al., 2019; Radford et al., 2019; Brown et al., 2020). Shifting the view to the field of modeling dynamical or even chaotic systems, encoder-decoder RNNs are still the method of choice for forecasting such continuous time series data (Wang et al., 2019; Thavarajah et al., 2021; Vlachas et al., 2018; Sehovac et al., 2019; Sehovac & Grolinger, 2020; Shen et al., 2020).

Nevertheless encoder-decoder RNNs do have their difficulties, especially when it comes to effectively training them. Firstly, there is the exposure bias issue that can appear when teacher forcing is used for training the model. Teacher forcing is the strategy that is typically applied when training RNNs for time series sequence-to-sequence tasks (Williams & Zipser, 1989) regardless of the type of data. To understand the problem we first give a quick side note about the motivation behind teacher forcing. Its main advantage is that it can

[1] To the reviewers: Upon deanonymization our code for the experiments will be made available as a replication package on Github. The datasets used in this paper were already published on Dataverse.

significantly reduce the number of steps a model needs to converge during training and improve its stability (Miao et al., 2020). However, teacher forcing may result in worse model generalization due to a discrepancy between training and testing data distribution. It is less resilient against self induced perturbations caused by prediction errors in the inference phase (Sangiorgio & Dercole, 2020). However, simply training the model without teacher forcing in free running mode instead does not necessarily provide convincing results as can be seen in Section 5.6. Rather a more sophisticated strategy is needed to guide the model through the training procedure.

Several authors propose methods to mitigate the exposure bias or improve training stability and results in general inventing certain strategies (Bengio et al., 2015; Nicolai & Silfverberg, 2020; Lamb et al., 2016; Liu et al., 2020; Dou et al., 2019). Even though, all these methods address the training for NLP tasks, such as text translation, text completion or image captioning, we focus on time series forecasting. Our datasets consist of sequences sampled from approximations of different chaotic systems. With these systems the next state can always be derived from the past state(s) deterministically but they also tend to be easily irritated by small perturbations. Thus the trained model needs to be especially resilient against small perturbations when auto-regressively predicting future values, otherwise those small errors will quickly accumulate to larger errors (Sangiorgio & Dercole, 2020). These aspects make the kind of data we use especially challenging. Since TF avoids the error accumulation only during training, we argue the models are even more vulnerable to issues like the exposure bias and will thus more likely fail to forecast larger horizons.

Around the interest of predicting particularly (chaotic) dynamical systems with RNNs another field has formed that very intensively studies several specialized RNN-based approaches proposed to stabilize the training process and prevent exploding gradients. Most of propositions include architectural tweaks or even new RNN architectures considering the specifics of dynamical systems and their theory (Lusch et al., 2018; Vlachas et al., 2018; Schmidt et al., 2019; Champion et al., 2019; Chang et al., 2019; Rusch & Mishra, 2020; Erichson et al., 2020; Rusch et al., 2021; Li et al., 2021).

Monfared et al. (2021), for example, performed a theoretical analysis relating RNN dynamics to loss gradients and argue that this analysis is especially insightful for chaotic systems. With this in mind they suggest a kind of sparse teacher forcing (STF) inspired by the work of Williams & Zipser (1989) that uses information about the degree of chaos of the treated dynamical system. As a result, they form a training strategy that is applicable without any architectural adaptations and without further hyperparameters. Their results using a vanilla RNN, a piecewise linear recurrent neural network (PLRNN) and an LSTM for the Lorenz (Lorenz, 1963) and the Rössler (Rössler, 1976) systems show clear superiority of applying chaos dependent STF.

Reservoir computing RNNs were successfully applied to chaotic system forecasting and analysis tasks as well. For example, Pathak et al. (2017) propose a reservoir computing approach that fits the attractor of chaotic systems and predicts their Lyapunov exponents.

In this paper, we focus on CL training strategies like scheduled sampling that require no architectural changes of the model and thus can be applied easily for different and existing sequence-to-sequence (seq2seq) models. All presented strategies will be evaluated across different benchmark datasets. Our main contributions are the following. First, assembling a set of training strategies for encoder-decoder RNNs that can be applied for existing seq2seq models without adapting their architecture. Second, presenting a collection of strategies' hyper-parameter configurations that optimize the performance of the trained model. Third proposing a "flipped classroom" like strategy that outperforms all existing comparable approaches on several datasets sampled from different chaotic systems. Fourth, proposing a method that yields substantially better prediction stability and therefore allows for forecasting longer horizons.

The course of the paper continues with Section 2 where we provide the background of sequence-to-sequence RNNs and the conventional ways to train them. We also give a short introduction to chaotic behavior of our data. In Section 3 we examine existing approaches dealing with the difficulty of training seq2seq RNNs in the context of different applications. Also, we give an overview of work treating RNNs for chaotic system prediction in particular. Section 4 describes how we designed our training strategies and how they are applied. Further information about the experimental setup and our results we present in Section 5. In Section 6 we discuss the results and the strengths and limitations of the different strategies. Finally, in Section 7 we conclude our findings.

2 Background

Within this paper, we study Curriculum Learning (CL) training strategies for sequence-to-sequence RNNs. We are using an encoder-decoder architecture (Chung et al., 2014) as model to forecast time series data. The rough structure of the encoder-decoder architecture is shown in Figure 1a. It consists of two separate RNNs, an encoder and a decoder. The encoder is trained to build up a hidden state representing the recent history of the processed time series. It takes an input sequence $(x_1, x_2, \ldots, x_n)$ of n input values where each value $x_j \in \mathbb{R}^d$ is a d dimensional vector. For each processed step the encoder updates its hidden state to provide context information for the following steps. The last encoder hidden state (after processing x_n) is then used as initial hidden state of the decoder. Triggered by a sequence's preceding value, the decoder's task is predicting its next future value while taking into account the sequence's history via the accumulated hidden state. For a trained network in the inference phase, that means that the decoders preceding prediction is auto-regressively fed back as input into the decoder (aka auto-regressive prediction) (cp. Fig. 1a). All m outputs $y_j \in \mathbb{R}^d$ together form the output sequence $(y_1, y_2, \ldots, y_m)$.

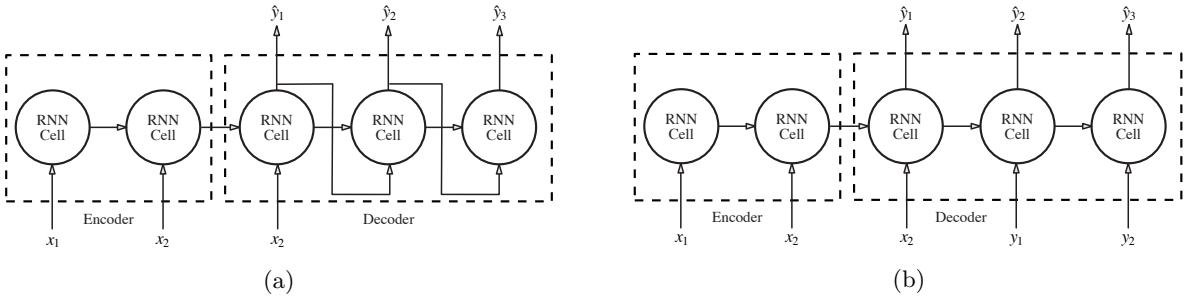

Figure 1: RNN encoder-decoder architecture in inference phase (a) and in training phase using teacher forcing (b)

2.1 Training Sequence Prediction Tasks

While training, the decoder's inputs may either be previous predicted outputs (free running) or known previous values stemming from the given dataset (teacher forcing). Training in free running mode might be an intuitive approach but slows down the training due to accumulated error throughout multiple prediction steps without the support of teacher forced inputs especially in the early training epochs (Nicolai & Silfverberg, 2020). In contrast, **teacher forcing** aims to avoid this problem by utilizing the corresponding previous ground truth value as decoder input rather than the previously predicted value. This way the model learns from the beginning of the training on to adapts its weights to perfect input values and converges Back noticeable faster (Miao et al., 2020) (cp. Fig. 1b). However, teacher forcing also bears a significant drawback since the model during training is never exposed to the noisy predicted values it will later face in the inference phase and it therefore does often not generalize very well. A model trained with teacher forcing solely learned to predict on basis of perfect values and is thus vulnerable for small perturbations on its input, this effect is called **exposure bias** (Ranzato et al., 2015).

2.2 Chaotic Systems

The data we are using for our experiments later in Section 5 is generated from chaotic systems. Whether or not a dynamical system is chaotic, can be confirmed by considering its Lyapunov exponents λ_k for $k \in [1, d]$. Given an initial perturbation ε_0 the exponential rate with which the perturbation will increase (or decrease) in the direction of dimension i is the Lyapunov exponent $\lambda_k = \lim_{t \to \infty} \frac{1}{t} \ln(\frac{||\varepsilon_t||}{||\varepsilon_0||})$ (Dingwell, 2006). That is, the Lyapunov exponents denote how sensitive the system is to the initial conditions (initial state). A deterministic dynamical system with at least one positive Lyapunov exponent while being aperiodic in its asymptotic limit is called **chaotic** (Dingwell, 2006). Analogously, dynamical systems with at least two positive, one negative, and one zero Lyapunov exponent are called **hyper-chaotic** systems. Dingwell points

out that the largest Lyapunov exponent (LLE) can be used as a measure to compare the chaotic behavior of different systems.

3 Related Work

Schmidt (2019) defines exposure bias as describing "a lack of generalization with respect to an – usually implicit and potentially task and domain dependent – measure other than maximum-likelihood" meaning that when the exclusive objective is to maximize the likelihood between the output and the target sequence one can use teacher forcing during training (Goodfellow et al., 2016). However, Goodfellow et al. argue that the kind of input the model sees while testing will typically diverge from the training data and the trained model may lack the ability of correcting its own mistakes. Thus, in practice the teacher forcing can be a proper training strategy but may hinder the model to learn compensating its inaccuracies. He et al. study exposure bias for natural language generation tasks (He et al., 2019). They use sequence and word level quantification metrics to observe the influence of diverging prefix distributions on the distribution of the generated sequences. Two distributions are generated. One with and one without induced exposure bias. Those two distributions are then compared on basis of the corresponding corpus-bleu scores (Papineni et al., 2002). The study concludes that for language generation the effect of the exposure bias is less serious than widely believed.

Several studies propose approaches to overcome the exposure bias induced by teacher forcing. The earliest of these studies proposes **scheduled sampling** (Bengio et al., 2015). Scheduled sampling tries to take the advantages of training with teacher forcing while also acclimating the trained model to its own generated data error. It does that by using ground truth values as input for a subset of the training steps and predicted values for the remaining. ϵ_i denotes the teacher forcing probability at step i. Accordingly, the probability of using the predicted value is $1 - \epsilon_i$. During training ϵ_i decreases from ϵ_s to ϵ_e. This procedure changes the input data while training, making it a curriculum learning approach, as which scheduled sampling was proposed and works without major architectural adaptions. Originally proposed for image captioning tasks, scheduled sampling was also applied, e.g., for sound event detection (Drossos et al., 2019). Nicolai and Silfverberg consider and study the teacher forcing probability ϵ as a hyperparameter. Rather than using a decay function that determines the decrease of ϵ_i over the course of training epochs, they use a fix teacher forcing probability throughout the training (Nicolai & Silfverberg, 2020). They observed a moderate improvement compared to strict teacher forcing training.Scheduled sampling is not restricted to RNN-based sequence-to-sequence models though, it has also been studied for transformer architectures (Mihaylova & Martins, 2019). Mihaylova and Martins tested their modified transformer on two translation tasks but could only observe improved test results for one of them.

Apart from scheduled sampling (Bengio et al., 2015), a number of approaches have been proposed typically aiming to mitigate the exposure bias problem by adapting model architectures beyond an encoder-decoder design. **Professor forcing** (Lamb et al., 2016) is one of these more interfering approaches that aims to guide the teacher forced model in training by embedding it into a Generative Adversarial Network (GAN) framework (Goodfellow et al., 2014). This framework consists of two encoder-decoder RNNs that form the generator and the discriminator respectively. The generating RNNs have shared weights that are trained with the same target sequence using their respective inputs while at the same time they try to fool the discriminator by keeping their hidden states and outputs as similar as possible. The authors conclude that their method, compared to teacher forcing, provides better generalization for single and multi step prediction. In the field of Text-To-Speech (TTS), the concept of professor forcing has also been applied in the GAN based training algorithm proposed by Guo et al. (2019). They adapted professor forcing and found that replacing the teacher forcing generator with one that uses scheduled sampling improved the results of their TTS model in terms of intelligibility. As another approach for TTS, (Liu et al., 2020) proposed **teacher-student training** using a training scheme to keep the hidden states of the model in free running mode close to those of a model that was trained with teacher forcing. It applies a compound objective function to align the states of the teacher and the student model. The authors observe improved naturalness and robustness of the synthesized speech compared to their baseline. Dou et al. (Dou et al., 2019) proposed attention forcing as yet another training strategy for sequence-to-sequence models relying on an attention mechanism that forces a reference attention alignment while training the model without teacher forcing. They studied TTS

tasks and observed a significant gain in quality of the generated speech. The authors conclude that attention forcing is especially robust in cases where the order of predicted output is irrelevant.

The discussed approaches for mitigating exposure bias were proposed in the context of NLP and mainly target speech or text generation. For time series forecasting, Sangiorgio & Dercole (2020) suggest to neglect teacher forcing completely and solely train the model in free running mode, thereby, sacrificing the faster convergence of teacher forcing and potentially not reaching convergence at all.

In the context of RNNs for forecasting and analyzing dynamical systems, the majority of existing work deals with exploding and vanishing gradients as well as capturing long-term dependencies while preserving the expressiveness of the network. Various studies rely on methods from dynamical systems theory applied to RNN or propose new network architectures.

Lusch et al. (2018) and Champion et al. (2019) use a modified autoencoder to learn appropriate eigenfunctions that the Koopman operator needs to linearize the nonlinear dynamics of the system. In another study, Vlachas et al. (2018) extend an LSTM model with a mean stochastic model to keep its state in the statistical steady state and prevent it from escaping the system's attractor. Schmidt et al. (2019) propose a more generalized version of a PLRNN (Koppe et al., 2019) by utilizing a subset of regularized memory units that hold information much longer and can thus keep track of long-term dependencies while the remaining parts of the architecture are designated to approximate the fast scale dynamics of the underlying dynamical system. The Antisymmetric Recurrent Neural Network (AntisymmetricRNN) introduced by Chang et al. (2019) represents an RNN designed to inherit the stability properties of the underlying ordinary differential equation (ODE) ensuring trainability of the network together with its capability of keeping track of long-term dependencies. A similar approach has been proposed as Coupled Oscillatory Recurrent Neural Networks (coRNNs) (Rusch & Mishra, 2020) that are based on a secondary order ODEs modeling a coupled network of controlled forced and damped nonlinear oscillators. The authors prove precise bounds of the RNN's state gradients and thus the ability of the coRNN being a possible solution for exploding or vanishing gradients. Erichson et al. (2020) propose the Lipschitz RNN having additional hidden-to-hidden matrices enabling the RNN to remain Lipschitz continuous. This stabilizes the network and alleviates the exploding and vanishing gradient problem. In Li et al. (2020; 2021), the authors propose the Fourier respectively the Markov neural operator that are built from multiple concatenated Fourier layers that directly work on the Fourier modes of the dynamical system. This way they retain major portion of the dynamics and forecast the future behavior of the system. Both, the incremental Recurrent Neural Network (IRNN) (Kag et al., 2019) and the time adaptive RNN (Kag & Saligrama, 2021) use additional recurrent iterations on each input to enable the model of coping different input time scales, where the latter provides a time-varying function that adapts the model's behavior to the time scale of the provided input.

All of this shows the increasing interest in the application of machine learning (ML) models for forecasting and analyzing (chaotic) dynamical systems. To meet this trend, Gilpin (2021) recently published a fully featured collection of benchmark datasets being related to chaotic systems including their mathematical properties.

A more general guide of training RNNs for chaotic systems is given by Monfared et al. (2021). They discuss under which conditions the chaotic behavior of the input destabilizes the RNN and thus leads to exploding gradients during training. As a solution they propose STF, where every τ-th time step a true input value is provided (teacher forced) as input instead of the previous prediction.

4 Teaching Strategies

Within this section, we systematically discuss existing teaching strategies for sequence-to-sequence prediction models and propose new strategies. All of these will then be evaluated in an experimental study with different time series reported in the following section.

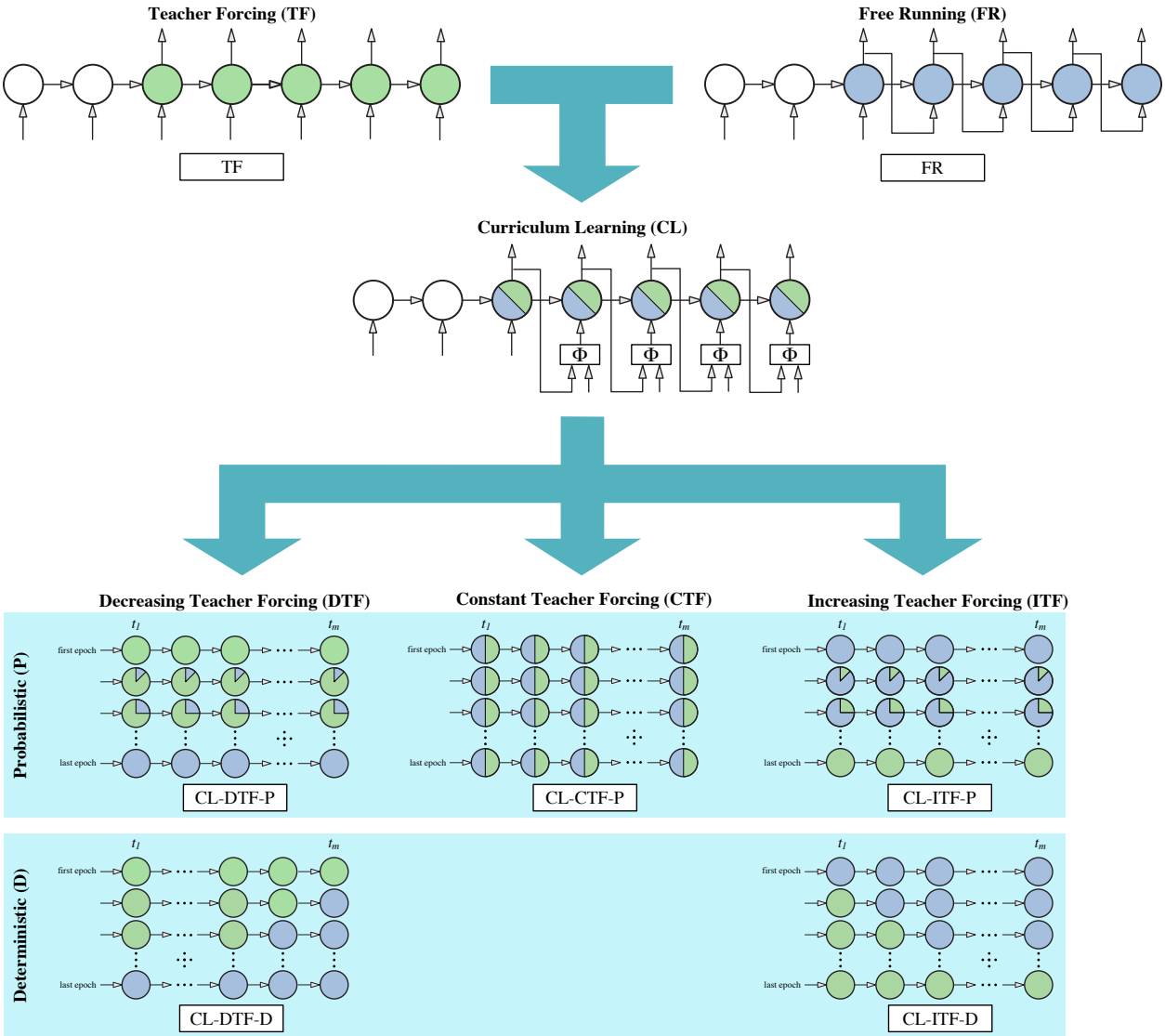

Figure 2: Overview of the proposed and evaluated training strategies where teacher forcing (TF) and free running (FR) refer to the two extreme cases that are combined to different CL strategies.

4.1 Free Running (FR) vs. Teacher Forcing (TF)

A widely used training strategy for RNN sequence-to-sequence models is to use teacher forcing (TF) throughout the whole training. Thereby, data is processed as shown in Fig. 2 (top left), i.e., the model is never exposed to its own predictions during training. A single forward step of the decoder during TF training is denoted as

$$\hat{y}^t = f(y^{t-1}, \theta, c^{t-1}), \tag{1}$$

where y^t is the ground truth value for time step t, $\hat{y}^t$ is the predicted value for time step t, θ denotes the trainable parameters of the model, and c^t is the decoder's hidden state at time step t.

The other extreme form of training is free running (FR), i.e., only the model's first output value is predicted on basis of ground truth input and all subsequent output values of the sequence are predicted on basis of previous predictions throughout the training (cp. Fig. 2 (top right)). A single forward step of the decoder during FR training is denoted as

$$\hat{y}^t = f(\hat{y}^{t-1}, \theta, c^{t-1}). \tag{2}$$

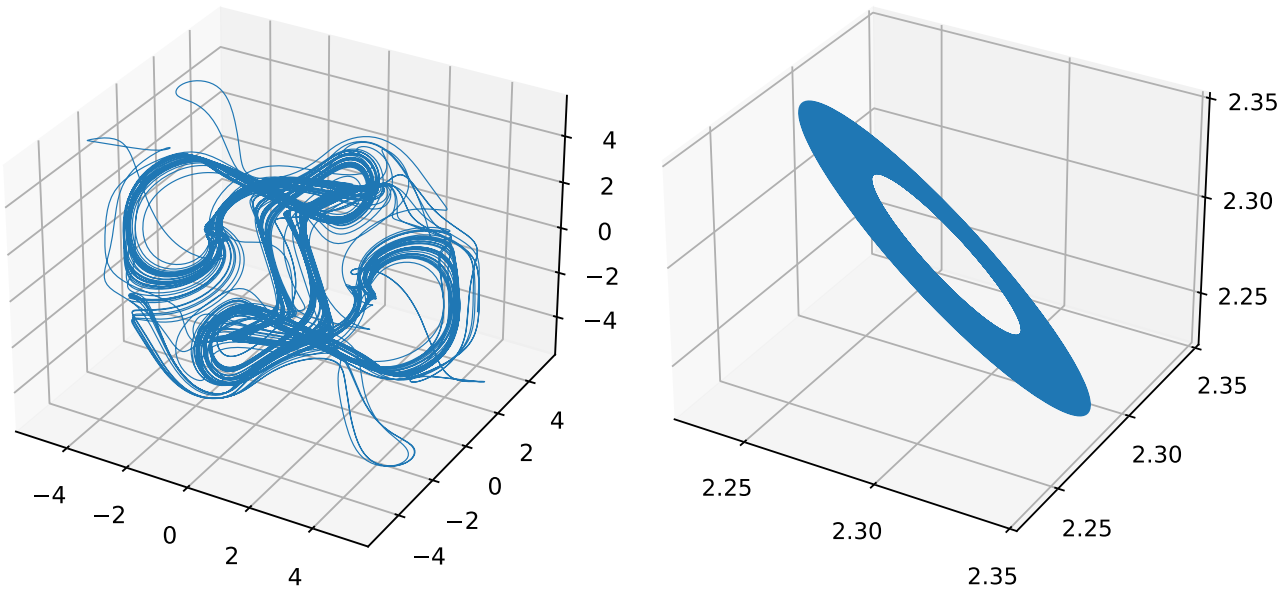

(a) (b)

Figure 3: 30 000 time steps sampled with a time delta of $dt = 0.1$ of Thomas' cyclically symmetric attractor in (a) a chaotic parametrization and (b) a periodic parametrization

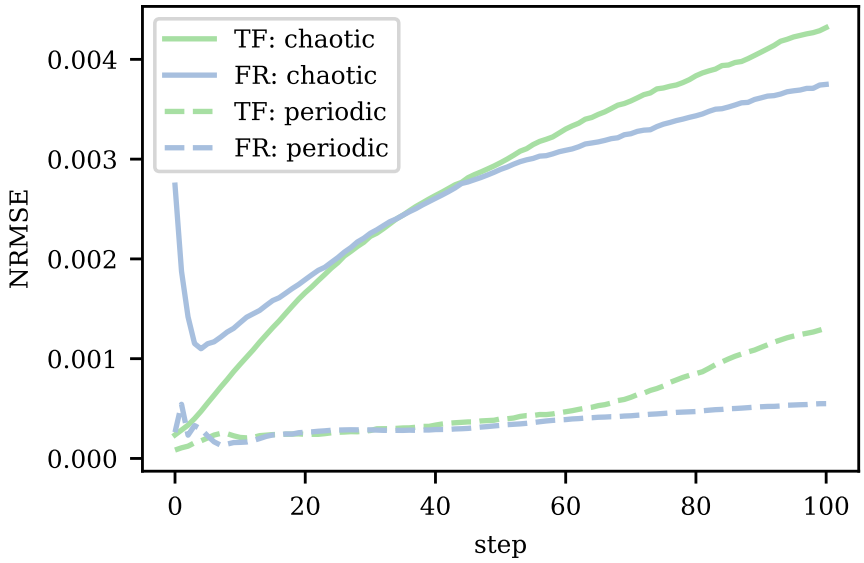

Figure 4: Test NRMSE over 100 predicted time steps of the chaotically and periodically parametrized Thomas attractor (cp. Fig. 3b), predicted by GRU models trained with teacher forcing (TF) and free running (FR).

A claimed major benefit of TF training is faster model convergence and thus reduced training time (Miao et al., 2020), while a major benefit of FR training is avoided exposure bias arising from solely training with ground truth data yielding a model that performs less robust on unseen validation data (Ranzato et al., 2015). To illustrate these benefits and drawbacks, we utilize the Thomas attractor with two parametrization, the first resulting in a periodic (cp. Fig. 3b) and the second resulting in a chaotic attractor (cp. Fig. 3a). By sampling from the attractors, we build two corresponding datasets of 10 000 samples each. For both datasets, we train a single layer encoder-decoder GRU following the free running (FR) and the teacher forcing (TF)

strategy. Figure 4 shows test Normalized Root Mean Squared Error (NRMSE) of per trained model over 100 predicted time steps. All models have been initialized with 150 ground truth values to build up the hidden state before predicting these 100 time steps. We observe that the chaotic variant is harder to predict for the trained models (cp. blue and green line in the figure) and that those trained with teacher forcing tend to predict with a smaller error at the first steps, which then grows relatively fast. In contrast, the prediction error of the FR trained models starts on a higher level but stays more stable over the prediction horizon. Arguing that time series forecasting represents an especially challenging task for sequence-to-sequence models when it exhibits chaotic behavior. The more precise forecasting capabilities of a TF-trained network at the early prediction steps vs. the overall more stable long-term prediction performance of a FR-trained network observed in the Thomas example (cp. Fig 3a, 3b), motivate the idea of combining both strategies into a CL approach.

Schmidt (2019) describes the exposure bias in natural language generation as a lack of generalization. Following this argumentation motivates an analysis of training with FR and TF strategies when applied to forecasting dynamical systems with different amounts of available training data. Figure 5 shows the NRMSE when forecasting the Thomas attractor using different dataset sizes and reveals that increasing the dataset size yields generally improved model performance for TF as well as FR, while their relative difference is maintained.

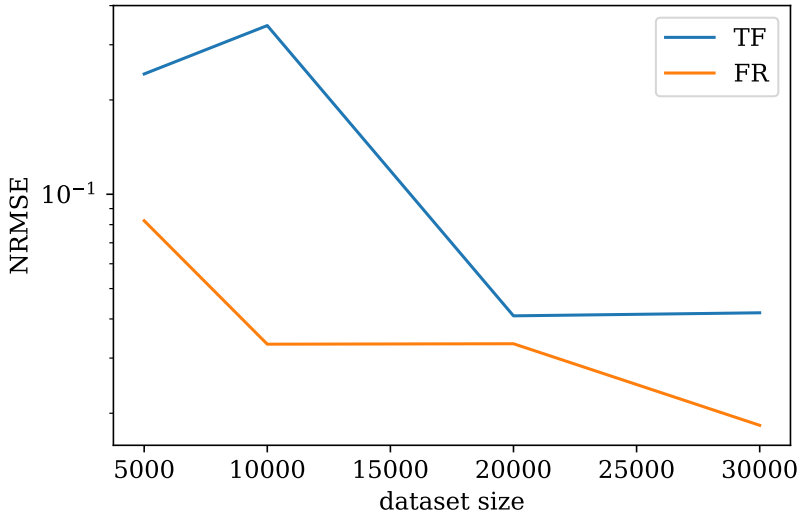

Figure 5: The NRMSE for different dataset sizes when using TF and FR during training for forecasting the Thomas attractor

4.2 Curriculum Learning (CL)

Within the context of our work, we denote the curriculum learning concept as combining teacher forcing and free running training, i.e., starting from the second decoder step the curriculum prescribes per decoder step whether to use the ground truth value or the predicted value of the previous time step as input. We formalize a single training step of a CL approach as follows:

$$\hat{y}^t = \begin{cases} f(y^{t-1}, \theta, c^{t-1}), & \text{if } \Phi = 1 \\ f(\hat{y}^{t-1}, \theta, c^{t-1}), & \text{otherwise} \end{cases} \tag{3}$$

where the teacher forcing decision Φ governs whether the decoder input is teacher forced or not. Figure 2 illustrates the data flow of a sequence-to-sequence model training with CL in between the conventional

strategies. In our naming scheme CL-DTF-P resembles the scheduled sampling approach proposed by Bengio et al. (2015). Below, we discuss the different types of curricula on training and iteration scale resulting in different ways for determining Φ.

4.3 Curriculum on Training Scale

The teacher forcing ratio ϵ_i per training iteration i is determined by a curriculum function $C : \mathbb{N} \rightarrow [0, 1]$ denoted as

$$\epsilon_i = C(i). \tag{4}$$

We distinguish three fundamental types of curriculum on training scale. First, constant curricula where a constant amount of teacher forcing is maintained throughout the training denoted as

$$\epsilon_i = \epsilon. \tag{5}$$

Second, decreasing curricula where the training starts with a high amount of teacher forcing that continuously declines throughout the training. Third, increasing curricula where the training starts at a low amount of teacher forcing that continuously increases throughout the training. Both follow a transition function $C : \mathbb{N} \rightarrow [\epsilon_{start}, \epsilon_{end}]$ denoted as

$$\epsilon_i = C(i), \tag{6}$$

where $\epsilon_{start} \leq \epsilon_i \leq \epsilon_{i+1} \leq \epsilon_{end}$ for increasing curricula, $\epsilon_{start} \geq \epsilon_i \geq \epsilon_{i+1} \geq \epsilon_{end}$ for decreasing curricula and $\epsilon_{start} \neq \epsilon_{end}$ for both. The following equations exemplary specify decreasing curricula (cp. Eqs. 7–9) following differing transition functions inspired by those used to study the scheduled sampling approach (Bengio et al., 2015)

$$\begin{aligned} C_{lin}(i) &= \max(\epsilon_{end}, \epsilon_{end} + (\epsilon_{start} - \epsilon_{end}) \cdot (1 - \frac{i}{Ł})), \\ &\quad \text{with } \epsilon_{end} < \frac{Ł - 1}{Ł}, \quad 1 < Ł, \quad i \in \mathbb{N}, \end{aligned} \tag{7}$$

$$\begin{aligned} C_{invSig}(i) &= \epsilon_{end} + (\epsilon_{start} - \epsilon_{end}) \cdot \frac{k}{k + e^{\frac{i}{k}}}, \\ &\quad \text{with } \epsilon_{end} < \epsilon_{start}, \quad 1 \leq k, \quad i \in \mathbb{N}, \end{aligned} \tag{8}$$

$$\begin{aligned} C_{exp}(i) &= \epsilon_{end} + (\epsilon_{start} - \epsilon_{end}) \cdot k^i, \\ &\quad \text{with } \epsilon_{end} < \epsilon_{start}, \quad 0 < k < 1, \quad i \in \mathbb{N}, \end{aligned} \tag{9}$$

where the curriculum length parameter Ł determines the pace as number of iterations which the curriculum C_{lin} needs to transition from ϵ_{start} to ϵ_{end}. The curricula C_{invSig} and C_{exp} have no such parameter since the functions never completely reach ϵ_{end} in theory. In practice though, we adapt the curriculum specific parameter k to stretch or compress these curricula along the iteration axis to achieve the same effect. Figure 6a exemplary visualizes three decreasing and three increasing curricula following differing transition functions C and being parametrized with $\epsilon_{start} = 1$ and $\epsilon_{end} = 0$ and $\epsilon_{start} = 0$ and $\epsilon_{end} = 1$ respectively. Furthermore, each is parametrized to have a curriculum length of Ł = 1 000. Figure 6b shows examples of decreasing and increasing C_{lin} with different Ł.

4.4 Curriculum on Iteration Scale

ϵ_i prescribes a ratio of TF vs. FR steps for a given training iteration i. Based on ϵ that solely prescribes the amount of teacher forcing for an iteration, we can now develop micro curricula for distributing the TF and FR steps eventually providing a teacher forcing decision Φ per training step. We propose two ways to distribute TF and FR steps within one training iteration: (1) probabilistic – where ϵ is interpreted as the probability of being a TF step, and (2) deterministic – where ϵ as a rate that determines the number of TF steps trained before moving to FR for the rest of the training sequence. For a probabilistic CL, we denote the teacher forcing decision Φ_ϵ, which is a discrete random variable that is drawn from a Bernoulli distribution:

$$\Phi_\epsilon \sim \text{Bernoulli}(\epsilon). \tag{10}$$

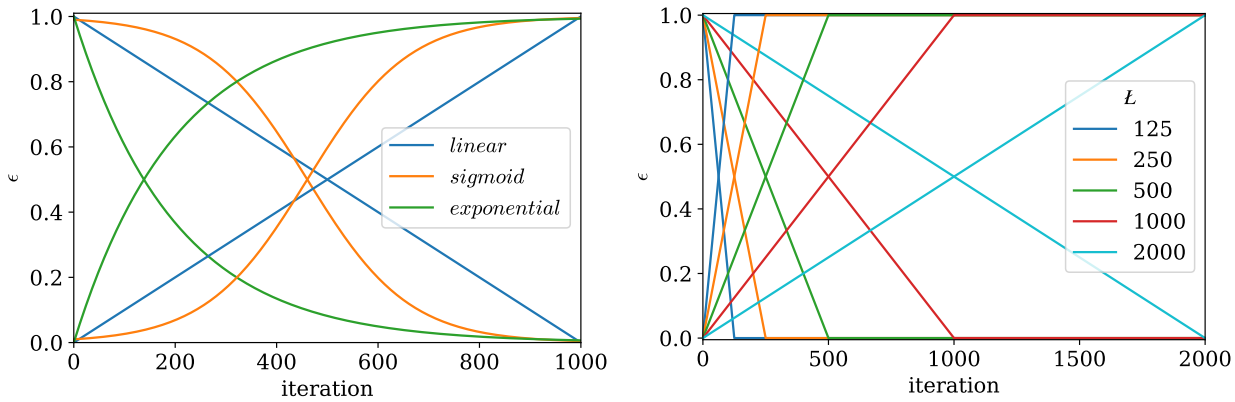

(a) (b)

Figure 6: Examples of different decreasing curricula and their corresponding increasing versions (a) and multiple linear curricula with different pace Ł (b).

For a deterministic CL, Φ depends not only on ϵ but also on the current position j within the predicted sequence of length m. Therefore, in this case we denote the teacher forcing decision $\Phi_{\epsilon,j}$ as:

$$\Phi_{\epsilon,j} = \begin{cases} 1, & \text{if } \epsilon \geq \frac{j}{m} \\ 0, & \text{otherwise.} \end{cases} \tag{11}$$

5 Evaluation

To compare the training strategies described in Section 4, we evaluate each with varying parametrization on six different datasets. Our experiments aim to answer the following six research questions:

RQ1 Baseline teaching strategies. How well and consistent do the current baseline strategies FR and TF train a model for forecasting dynamical systems?

RQ2 Curriculum learning strategies. How do the different curriculum learning strategies perform in comparison to the baseline strategies?

RQ3 Training length. How is training length influenced by the different teaching strategies?

RQ4 Prediction stability. How stable is a model's prediction performance over longer prediction horizons when trained with the different strategies?

RQ5 Curriculum parametrization. How much does the curriculum's parametrization influence model performance?

RQ6 Iteration scale curriculum. How do iteration scale curricula differ in resulting model performance?

5.1 Evaluated Curricula

In total, we define eight strategies that we evaluate in this study (cp. Fig. 2). For comparison, we train the two baseline methods teacher forcing (TF) and free running (FR) that "teach" throughout the entire training or do not "teach" at all respectively. All other methods prescribe a teaching curriculum CL throughout the training and we distinguish these strategies along two dimensions: (1) the overall increasing (ITF), constant (CTF), or decreasing (DTF) trend in teacher forcing throughout the training curriculum and (2) the probabilistic (P) or deterministic (D) teacher forcing distribution within training steps.

Table I: Curriculum strategy parameters used during the *baseline*, *exploratory*, and the *essential* experiments

	Strategy	Curriculum parameter	Curriculum evaluated values
baseline	FR	C	–
		ϵ	0.0
		Ł	–
	TF	C	–
		ϵ	1.0
		Ł	–
exploratory	CL-CTF-P	C	–
		ϵ	$\{0.25, 0.5, 0.75\}$
		Ł	–
	CL-DTF-P, CL-DTF-D	C	$\{\text{linear}, \text{inverse sigmoid}, \text{exponential}\}$
		$\epsilon_{start} \rightarrow \epsilon_{end}$	$\{0.25, 0.5, 0.75, 1.0\} \rightarrow\ 0.0$
		Ł	1000
	CL-ITF-P, CL-ITF-D	C	$\{\text{linear}, \text{inverse sigmoid}, \text{exponential}\}$
		$\epsilon_{start} \rightarrow \epsilon_{end}$	$\{0.0, 0.25, 0.5, 0.75\} \rightarrow\ 1.0$
		Ł	1000
essential	CL-DTF-P, CL-DTF-D, CL-ITF-P, CL-ITF-D	C	linear
		$\epsilon_{start} \rightarrow \epsilon_{end}$	$\{0.0 \rightarrow 1.0, 1.0 \rightarrow 0.0\}$
		Ł	$\{62, 125, 250, 500, 1\,000, 2\,000, 4\,000, 8\,000, 16\,000, 32\,000\}$

5.2 Parametrization of Training Curricula

Table I shows all training strategy-specific parameters and their values for the evaluated strategies. We subdivide our experiments into three sets: *baseline*, *exploratory*, and *essential* experiments. The baseline strategies FR and TF do not have any additional parameters. The CL-CTF-P strategy has the ϵ parameter configuring the strategy's teacher forcing ratio. The increasing and decreasing strategies CL-DTF-x and CL-ITF-x are configured by ϵ_{start} and ϵ_{end} referring to the initial and eventual amount of teacher forcing and the function C transitioning between both. Additionally, Ł determines the number of training epochs in between ϵ_{start} and ϵ_{end}. For the *exploratory* experiments, we utilize a fix Ł $= 1\,000$, while for the *essential* experiments, we evaluate all strategies solely using a linear transition C_{linear} in the curriculum (cp. Eq. 7) with either $\epsilon_{start} = 0$ and $\epsilon_{end} = 1$ (increasing) or $\epsilon_{start} = 1$ and $\epsilon_{end} = 0$ (decreasing).

5.3 Performance Metrics

We use the NRMSE and the R^2 metrics as well as two derived of those to evaluate model performance. NRMSE is a normalized version of the Root Mean Squared Error (RMSE) where smaller values indicate better prediction performance. For a single value of a sequence, NRMSE is calculated as:

$$\text{NRMSE}(y, \hat{y}) = \frac{\sqrt{\frac{1}{d} \cdot \sum_{j=1}^{d} (y_j - \hat{y}_j)^2}}{\sigma}, \tag{12}$$

where y is a ground truth vector, $\hat{y}$ is the corresponding prediction, $\sigma$is the standard deviation across the whole dataset, and d is the size of the vectors y and $\hat{y}$. For model evaluation, we calculate the mean NRMSE over all m forecasted steps of a sequence. Additionally, we compute and report the NRMSE only for the last $\left\lceil \frac{m}{10} \right\rceil$ forecasted steps of a sequence to specifically evaluate model performance at long prediction horizons.

The R^2 score lies in the range $(-\infty, 1]$ with higher values referring to better prediction performance. A score of 0 means that the prediction is as good as predicting the ground truth sequence's mean vector $\bar{y}$. The R^2

Table II: Details of the chaotic systems that were approximated to generate the data used for our experiments

System	**ODE/DDE**	**Parameters**	d	**LLE**
Mackey-Glass	$\frac{dx}{dt} = \beta \frac{x_\tau}{1+x_\tau^n} - \gamma x$ with $\gamma, \beta, n > 0$	$\tau = 17$, $n = 10$, $\gamma = 0.1$ $\beta = 0.2$, $dt = 1.0$	1	0.006
Thomas	$\frac{dx}{dt} = sin(y) - bx$ $\frac{dy}{dt} = sin(z) - by$ $\frac{dz}{dt} = sin(x) - bz$	$b = 0.1$, $dt = 0.1$	3	0.055
Rössler	$\frac{dx}{dt} = -(y+z)$ $\frac{dy}{dt} = x + ay$ $\frac{dz}{dt} = b + z(x-c)$	$a = 0.2$, $b = 0.2$ $c = 5.7$, $dt = 0.12$	3	0.069
Hyper Rössler	$\frac{dx}{dt} = -y - z$ $\frac{dy}{dt} = x + ay + w$ $\frac{dz}{dt} = b + xz$ $\frac{dw}{dt} = -cz + dw$	$a = 0.25$, $b = 3$ $c = 0.5$, $d = 0.05$ $dt = 0.1$	4	0.14
Lorenz	$\frac{dx}{dt} = -\sigma x + \sigma y$ $\frac{dy}{dt} = -xz + \rho x - y$ $\frac{dz}{dt} = xy - \beta z$	$\sigma = 10$, $\beta = \frac{8}{3}$ $\rho = 28$, $dt = 0.01$	3	0.905
Lorenz'96	$\frac{dx_k}{dt} = -x_{k-2}x_{k-1} + x_{k-1}x_{k+1} - x_k + F$ for $k = 1 \dots d$ and $x_{-1} = x_d$	$F = 8$, $dt = 0.05$	40	1.67

score is computed as:

$$R^2 = 1 - \frac{\sum_{j=1}^{d}(y_j - \hat{y}_j)^2}{\sum_{j=1}^{d}(y_j - \bar{y}_j)^2}. \tag{13}$$

We use the R^2 score to compute another metric LT$R^2 > 0.9$ measuring the number of Lyapunov Time (LT)s that a model can predict without the R^2 score dropping below a certain a threshold of 0.9. Sangiorgio and Dercole (Sangiorgio & Dercole, 2020) proposed this metric while applying a less strict threshold of 0.7.

5.4 Evaluated Datasets

We use six different time series datasets that we built by approximating six commonly studied chaotic systems (cp. Tab. II), i.e., Mackey-Glass (Mackey & Glass, 1977), Rössler (Rössler, 1976), Thomas' cyclically symmetric attractor (Thomas, 1999), Hyper Rössler (Rossler, 1979), Lorenz (Lorenz, 1963) and Lorenz'96 (Lorenz, 1996). Table II shows per system, the differential equations and how we parametrized them. These systems, differ among other in the number of dimensions d and degree of chaos as indicated by the largest lyapunov exponent in the LLE column of Tab. II. The LLEs are approximated values that were published independently in the past (Brown et al., 1991; Sprott & Chlouverakis, 2007; Sano & Sawada, 1985; Sandri, 1996; Hartl, 2003; Brajard et al., 2020). We generate datasets by choosing an initial state vector of size d and approximate 10 000 samples using the respective differential equations. We use SciPy package's implementation of the Livermore solver for ordinary differential equations (LSODE) (Radhakrishnan & Hindmarsh, 1993) except for Mackey-Glass which we approximate through the Python module JiTCDDE implementing the delayed differential equation (DDE) integration method proposed by (Shampine & Thompson, 2001). Thereby, dt defines the time difference between two sampled states per dataset and is shown in Table II. Where available, we chose dt similar to previous studies aiming for comparability of results. We split each dataset into 80% training samples and 10% validation and testing samples respectively. All data is normalized following a z-transform.

Table III: Results of the *exploratory* tests with the best hyperparameter configuration per strategy and system. The arrow besides each metric's column title indicates whether smaller (↓) or larger (↑) values are favored. The best result values per dataset are printed in bold and the best baseline NRMSEs are underlined. Together with each dataset we put the corresponding LLE in parenthesis.

		Best performing curriculum		Trained	NRMSE over 1LT			
	Strategy	C	ϵ	**epochs**	**absolut ↓**	**rel. impr. ↑**	**@BL epoch ↓**	**last 10% ↓**
Thomas (0.055)	FR	constant	0.00	427	<u>0.03416</u>	–	–	0.047222
	TF	constant	1.00	163	0.34545	–	–	0.607954
	CL-CTF-P	constant	0.25	450	0.05535	−62.03%	0.05675	0.082443
	CL-DTF-P	inverse sigmoid	0.75 ↘ 0.00	598	0.01858	45.61%	0.02120	0.034325
	CL-DTF-D	exponential	0.25 ↘ 0.00	557	0.03229	5.47%	0.03792	0.039749
	CL-ITF-P	exponential	0.00 ↗ 1.00	620	0.01403	58.93%	**0.02026**	0.026014
	CL-ITF-D	exponential	0.25 ↗ 1.00	944	**0.01126**	**67.04%**	0.02179	**0.018571**
Rössler (0.069)	FR	constant	0.00	3 863	<u>0.00098</u>	–	–	0.000930
	TF	constant	1.00	500	0.00743	–	–	0.016119
	CL-CTF-P	constant	0.25	2 081	0.00084	14.29%	0.00084	0.001333
	CL-DTF-P	linear	1.00 ↘ 0.00	2 751	0.00083	15.31%	0.00083	0.000931
	CL-DTF-D	inverse sigmoid	0.25 ↘ 0.00	4 113	0.00064	34.69%	0.00066	0.000578
	CL-ITF-P	inverse sigmoid	0.00 ↗ 1.00	7 194	0.00025	74.49%	0.00034	**0.000358**
	CL-ITF-D	linear	0.75 ↗ 1.00	5 132	**0.00024**	**75.51%**	**0.00031**	0.000390
Lorenz (0.905)	FR	constant	0.00	918	0.01209	–	–	0.013166
	TF	constant	1.00	467	<u>0.00152</u>	–	–	0.002244
	CL-CTF-P	constant	0.75	297	0.00167	−9.87%	0.00167	0.002599
	CL-DTF-P	inverse sigmoid	0.75 ↘ 0.00	522	0.00168	−10.53%	0.00162	0.002425
	CL-DTF-D	inverse sigmoid	1.00 ↘ 0.00	204	0.00187	−23.03%	0.00187	0.002823
	CL-ITF-P	linear	0.00 ↗ 1.00	750	0.00149	1.97%	0.00217	0.002235
	CL-ITF-D	inverse sigmoid	0.75 ↗ 1.00	803	**0.00124**	**18.42%**	**0.00132**	**0.002084**
Lorenz'96 (1.67)	FR	constant	0.00	8 125	0.07273	–	–	0.126511
	TF	constant	1.00	4 175	<u>0.03805</u>	–	–	0.075583
	CL-CTF-P	constant	0.50	2 615	0.07995	−110.12%	0.07995	0.140700
	CL-DTF-P	linear	0.75 ↘ 0.00	939	0.04654	−22.31%	0.04654	0.087228
	CL-DTF-D	linear	0.75 ↘ 0.00	1 875	0.04381	−15.14%	0.04381	0.081025
	CL-ITF-P	inverse sigmoid	0.25 ↗ 1.00	4 787	**0.01854**	**51.27%**	**0.02016**	**0.036651**
	CL-ITF-D	inverse sigmoid	0.00 ↗ 1.00	3 263	0.02093	44.99%	0.02196	0.040356

5.5 Training Procedure

All evaluated models follow an encoder-decoder GRU architecture with an additional fully connected layer after the decoder (cp. Fig. 7). We performed a full grid search for the hyper-parameters learning rate, batch size, learning rate reduction factor, loss plateau, input length n and hidden state size to determine suitable configurations for the experiments. Based on this optimization, we used the Adam (Kingma et al., 2015) optimizer with a batch size of 128 and apply Reduce Learning Rate on Plateau (RLROP) with an initial learning rate of $1e^{-3}$ and a reduction factor of 0.6, i.e., 40% learning rate reduction, given a loss plateau of 10 epochs for all datasets except Lorenz'96 where we use a reduction factor of 0.9 and a 20 epoch plateau respectively. Furthermore, we found an input length of $n = 150$ steps and a *hidden state size* of 256 to be most suitable. We use early stopping with a *patience* of 100 epochs and a *minimum improvement threshold* of 1% to ensure the convergence of the model while preventing from overfitting. We train all models with a dataset-specific prediction length m defined as:

$$m = \left\lceil \frac{\mathrm{LT}}{dt} \right\rceil = \left\lceil \frac{1}{dt \cdot \mathrm{LLE}} \right\rceil. \tag{14}$$

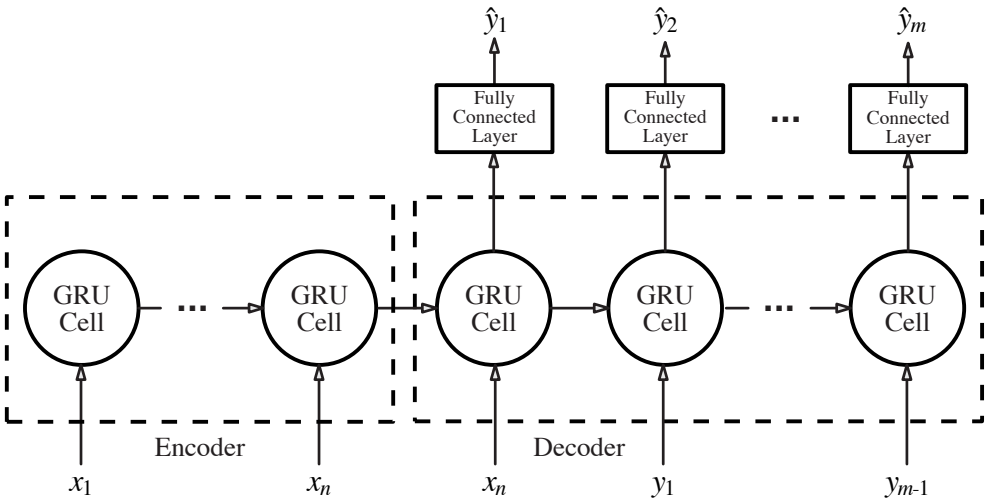

Figure 7: Structure of a simple encoder-decoder GRU used for training with teacher forcing

The reason being that we aim to train for the same forecasting horizon that we mainly evaluate a trained model with. We adapt this horizon to the dataset's LT thereby aiming for performance measures that are comparable across datasets.

We provide plots of the training and validation loss curves of the final parametrization per strategy and dataset in Appendix A. Based on these loss curves, we observe for ITF in contrast to DTF strategies that the training loss tends to move away from the validation loss faster. This is explainable by the fact that with increasing training time ITF strategies deliver an increasing amount of TF inputs counteracting the accumulation of error along the forecasted sequence and therefore further reducing training loss. For DTF strategies we observe an opposing behavior. Regarding training iterations, we observe that ITF strategies typically train for a larger number of epochs. Following the teacher forcing ratio curve (ϵ) we see that even when the increasing curriculum already arrived at the final $\epsilon_e = 1.0$, which means that it is using solely TF training from there on, it can improve for many more epochs than by simply using TF from the beginning. Since the termination of the training is determined by the early stopping criterion this shows that ITF may facilitate a longer and (regarding the validation loss) typically more successful training process compared to DTF and baseline strategies. We show the corresponding curves exemplary for the Rössler training in Figure 8.

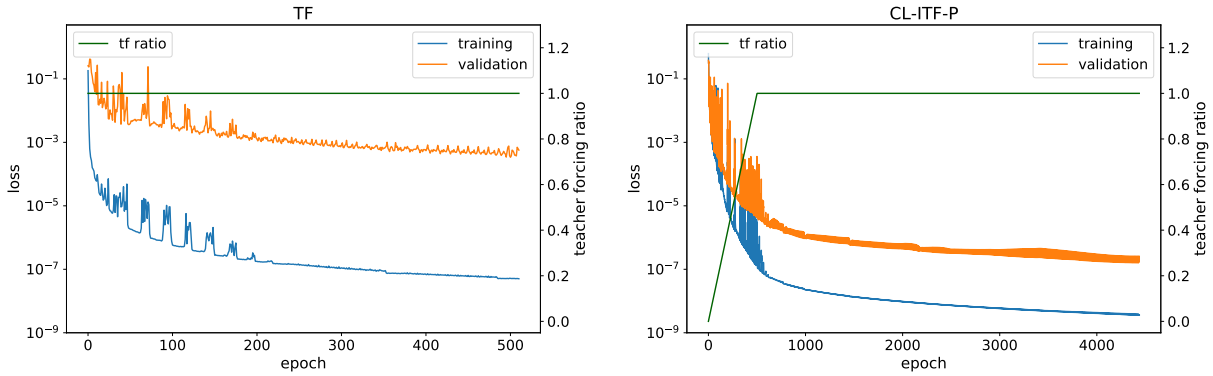

(a) (b)

Figure 8: Loss and teacher forcing ratio curves for Rössler

Table IV: Best curriculum length per strategy and system for all six datasets. The arrow besides a metric's column title indicates whether smaller (↓) or larger (↑) values are favored. The best result values per dataset are printed in bold and the best baseline NRMSEs are underlined. Together with each dataset we put the corresponding LLE in parenthesis.

	Strategy	Best performing curriculum ϵ	Ł	Trained epochs	NRMSE over 1LT absolut↓	rel. impr.↑	@BL epoch↓	last 10%↓	#LT with $R^2 > 0.9$ ↑
Mackey Glass (0.006)	FR	0.00	–	4 713	<u>0.00391</u>	–	0.00391	0.004101	4.50
	TF	1.00	–	44	0.09535	–	0.09535	0.171945	1.64
	CL-CTF-P	0.25	–	2 918	0.00632	−61.64%	0.00632	0.006544	4.51
	CL-DTF-P	1.00 ↘ 0.00	2 000	3 733	0.00215	45.01%	0.00215	0.003010	4.95
	CL-DTF-D	1.00 ↘ 0.00	1 000	431	0.00585	−49.62%	0.00585	0.011022	3.91
	CL-ITF-P	0.00 ↗ 1.00	500	1 566	**0.00104**	**73.40%**	**0.00104**	**0.001793**	**5.18**
	CL-ITF-D	0.00 ↗ 1.00	500	1 808	0.00211	46.03%	0.00211	0.003032	4.99
Thomas (0.055)	FR	0.00	–	427	<u>0.03416</u>	–	0.03416	0.047222	2.04
	TF	1.00	–	163	0.34545	–	0.34545	0.607954	1.73
	CL-CTF-P	0.25	–	450	0.05535	−62.03%	0.05675	0.082443	1.53
	CL-DTF-P	1.00 ↘ 0.00	1 000	356	0.05084	−48.83%	0.05084	0.105585	2.13
	CL-DTF-D	1.00 ↘ 0.00	1 000	326	0.10712	−213.58%	0.10712	0.206923	1.53
	CL-ITF-P	0.00 ↗ 1.00	500	677	**0.00930**	**72.78%**	**0.01645**	**0.016729**	**3.99**
	CL-ITF-D	0.00 ↗ 1.00	500	649	0.01819	46.75%	0.03934	0.030589	2.05
Rössler (0.069)	FR	0.00	–	3 863	<u>0.00098</u>	–	0.00098	0.000930	9.46
	TF	1.00	–	500	0.00743	–	0.00743	0.016119	4.75
	CL-CTF-P	0.25	–	2 081	0.00084	14.29%	0.00084	0.001333	7.51
	CL-DTF-P	1.00 ↘ 0.00	1 000	2 751	0.00083	15.31%	0.00083	0.000931	8.46
	CL-DTF-D	1.00 ↘ 0.00	125	4 879	0.00100	−2.04%	0.00116	0.000947	9.28
	CL-ITF-P	0.00 ↗ 1.00	500	4 523	**0.00019**	**80.61%**	**0.00022**	**0.000303**	**10.23**
	CL-ITF-D	0.00 ↗ 1.00	4 000	7 267	0.00027	72.24%	0.00051	0.000368	9.41
Hyper Rössler (0.14)	FR	1.00	–	6 461	0.00599	–	0.00599	0.007011	6.57
	TF	0.00	–	2 788	<u>0.00435</u>	–	0.00762	0.011194	5.24
	CL-CTF-P	0.25	–	2 909	0.01450	−233.33%	0.01450	0.015944	5.21
	CL-DTF-P	1.00 ↘ 0.00	2 000	3 773	0.00560	28.74%	0.00560	0.007052	6.32
	CL-DTF-D	1.00 ↘ 0.00	16 000	1 793	0.00490	12.64%	0.00490	0.007471	6.30
	CL-ITF-P	0.00 ↗ 1.00	125	2 802	0.00366	15.86%	0.00366	0.005802	6.50
	CL-ITF-D	0.00 ↗ 1.00	250	3 317	**0.00326**	**25.06%**	**0.00326**	**0.004639**	**6.72**
Lorenz (0.905)	FR	0.00	–	918	0.01209	–	0.01319	0.013166	3.31
	TF	1.00	–	467	<u>0.00152</u>	–	0.00152	0.002244	6.72
	CL-CTF-P	0.75	–	297	0.00167	−9.87%	0.00167	0.002599	6.43
	CL-DTF-P	1.00 ↘ 0.00	4 000	450	0.00124	18.42%	**0.00124**	0.001925	6.64
	CL-DTF-D	1.00 ↘ 0.00	16 000	587	0.00111	26.97%	0.00127	0.001650	6.53
	CL-ITF-P	0.00 ↗ 1.00	250	1 137	**0.00060**	**60.53%**	**0.00124**	**0.000883**	**7.19**
	CL-ITF-D	0.00 ↗ 1.00	250	578	0.00135	11.18%	0.00189	0.001725	4.33
Lorenz'96 (1.67)	FR	0.00	–	8 125	0.07273	–	0.08362	0.126511	2.34
	TF	1.00	–	4 175	<u>0.03805</u>	–	0.03805	0.075583	3.01
	CL-CTF-P	0.50	–	2 615	0.07995	−110.12%	0.07995	0.140700	2.25
	CL-DTF-P	1.00 ↘ 0.00	1 000	983	0.05278	−38.71%	0.05278	0.098130	2.67
	CL-DTF-D	1.00 ↘ 0.00	1 000	4 083	0.07119	−87.10%	0.07119	0.126636	2.34
	CL-ITF-P	0.00 ↗ 1.00	250	3 886	0.01680	55.85%	0.01680	0.032439	4.01
	CL-ITF-D	0.00 ↗ 1.00	250	3 379	**0.01628**	**57.21%**	**0.01628**	**0.031464**	**4.18**

5.6 Results

Table III shows results for the *exploratory* experiments. Per evaluated strategy and dataset, the table reports resulting model performance in terms of NRMSE. We only report that curriculum configuration in terms of transition function C and ϵ schedule that yields the highest NRMSE per strategy and dataset. Each model was used to predict a dataset-spetefic horizon of 1 LT. The best result per dataset and performance metric is highlighted in bold. First, we study the baseline strategies FR and TF and observe that for two datasets, i.e., Thomas and Rössler, the FR strategy outperforms the TF baseline, while TF outperforms FR for the other two. We select the one that performs best per dataset to measure relative improvement or deterioration gained by training with the respective curriculum learning strategy (cp. column "NMRSE rel.

impr."). We observe that across all datasets and performance metrics the CL-ITF-P and CL-ITF-D strategies yield the best and second best performing model with a relative improvement of 1.97 – 80.61% over the best performing baseline strategy. The other curriculum learning strategies perform less consistent across the datasets. The CL-DTF-x strategies yield an improved NRMSE for half of the datasets while the constant CL-CTF-P only yields an improvement for the Thomas attractor. We separately report the NRMSE of the last 10% predicted values of 1 LT test horizon per dataset to assess how robust a prediction is over time (cp. column "NRMSE last 10%"). We observe that the CL-ITF-P and CL-ITF-D strategies also reach the best performance in terms of this metric meaning that they yield the most robust models. We further observe a diverse set of curriculum configurations yielding the best performing model per strategy and dataset. That means that all available transition functions, i.e., linear, inverse sigmoid, and exponential, have been discovered as best choice for at least one of the trained models. Further, we observe all evaluated ϵ as best choice for the CL-CTF-P strategy and one of the datasets respectively. Similarly, the best performing initial ϵ for the increasing and decreasing transitions per dataset spans all evaluated values except for 0.5. The table also reports the number of training iterations till reaching the early stopping criterion (cp. column "training epochs"). We observe that the two baseline strategies utilize strongly differing numbers of iterations across all datasets. For the Thomas and the Rössler attractor, the teacher forcing strategy TF does not allow for proper model convergence being characterized by a low number of iterations and a high NRMSE compared to the other strategies. Among the curriculum teaching strategies across all datasets, the strategies with increasing teacher forcing ratio CL-ITF-x utilize the most training iterations. These CL-ITF-x strategies also utilize more training iterations than the better performing baseline strategy across all datasets. To better understand whether the longer training is the sole reason for the higher performance of the CL-ITF-x trained models, we additionally report the performance in terms of NRMSE of all curriculum trained models after the same number of training iterations as the better performing baseline model, i.e., after 427 epochs for Thomas, after 3 863 epochs for Rössler, after 467 epochs for Lorenz, and after 4 175 epochs for Lorenz'96 (cp. column "Performance @BL epochs"). We observe across all datasets that the best performing teaching strategy still remains CL-ITF-P or CL-ITF-D. In conclusion, the *exploratory* experiments demonstrated that a well-parametrized CL-ITF-x strategy yields a 18.42 – 75.51% performance increase across the evaluated datasets.

However, this improvement comes at the cost of an intensive parameter optimization of the respective curriculum. Therefore, we run a second series of *essential* experiments in which we simplify the parametrization of the curriculum by utilizing a linear transition from either $0.0 \rightarrow 1.0$ (CL-ITF-x) or $1.0 \rightarrow 0.0$ (CL-DTF-x) that is solely parametrized by the length of this transition in terms of training epochs Ł. Table IV reports results in terms of the previously introduced performance metrics again measured over a prediction horizon of 1 LT and across the same teaching strategies for six datasets including those studied for the *exploratory* experiments. Since the changes of the *essential* over the *exploratory* experiments solely effect teaching strategies with a training iteration-dependent curriculum, they have no effect on the baseline strategies FR and TF as well as the constant curriculum CL-CTF-P, which we still report in Table IV for direct comparison. Overall, we observe that CL-ITF-P outperforms all other strategies for four out of six datasets while it performs second best for the remaining two datasets where the deterministic version CL-ITF-D performs best. These strategies yield relative improvements ranging from 25.06 – 80.61% and are, thus, even higher than those observed for the *exploratory* experiments. Beyond that we observe that for all datasets treated in both experimental sets, the training curricula used in the *essential* experiments yield better performing models. For three out of four datasets the training even requires substantially less training iterations than in the explorative experiments. Additionally, we report in column "#LT with $R^2 > 0.9$" the prediction horizon in terms of LT that a trained model can predict while constantly maintaining an $R^2 > 0.9$. We observe that the ranking between the different strategies mostly remains the same as those observed when predicting 1 LT. That means that also the best performing strategy consistently remains the same for the longer horizon. Figure 9 more concretely depicts how the R^2 score develops across the prediction horizon for the different teaching strategies and datasets.

5.7 Additional Experiments

Judging from the essential experiments CL-ITF-x are our winning strategies on the datasets we tested. However, as mentioned in Section 3 there are many other approaches that predict chaotic systems with

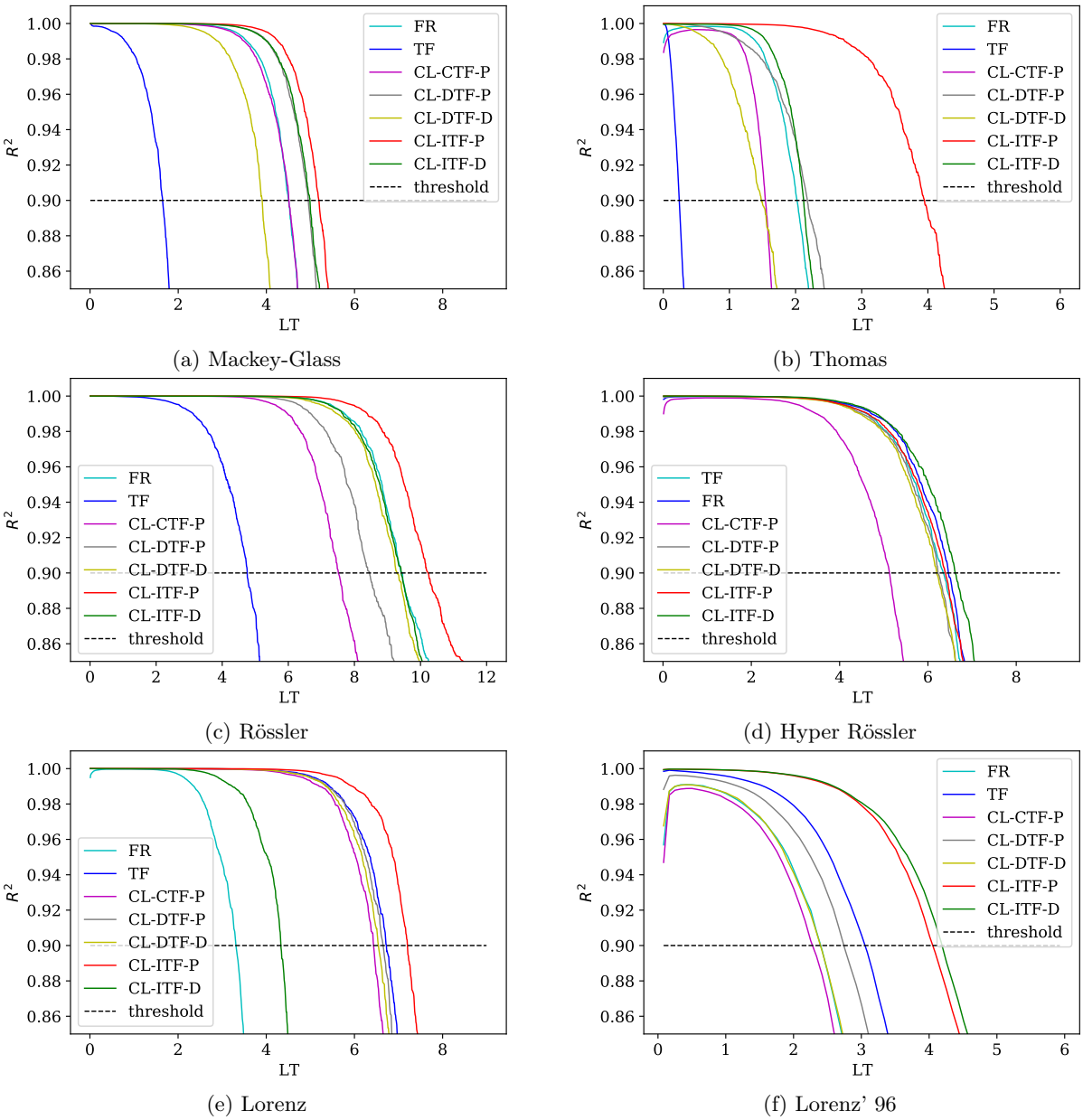

(a) Mackey-Glass

(b) Thomas

(c) Rössler

(d) Hyper Rössler

(e) Lorenz

(f) Lorenz' 96

Figure 9: R^2 score over multiple LTs for the six studied datasets using eight different training strategies

adapted RNNs architectures that take theoretical insights of dynamical systems into account. STF (Monfared et al., 2021) does not require any architectural modifications but instead provides an adapted training strategy. It determines a time interval $\tau = \frac{ln2}{LLE}$ that denotes how many FR steps are processed before the next TF value is used within one sequence. We find this strategy comparable to the CL approaches we study. Therefore, we execute another set of experiments where we use STF during the training of our encoder-decoder GRU for all chaotic systems in Table II. Since our data is sampled with different dt we have to redefine the time interval as $\tau = \frac{ln2}{LLE \cdot dt}$.

Table V: Results of STF with those of the baseline and the CL-ITF-x strategies

System	**Strategy**	**Epochs**	**NRMSE ↓**	**Rel. impr. ↑**
Mackey-Glass (0.006)	FR	4 713	<u>0.00391</u>	–
	TF	44	0.09535	–
	CL-ITF-P	1 566	0.00104	73.40%
	CL-ITF-D	1 808	**0.00211**	46.03%
	STF	5 517	0.00254	35.04%
Thomas (0.055)	FR	427	<u>0.03416</u>	–
	TF	163	0.34545	–
	CL-ITF-P	677	**0.00930**	72.78%
	CL-ITF-D	649	0.01819	46.75%
	STF	432	0.03655	−7.00%
Rössler (0.069)	FR	3 863	<u>0.00098</u>	–
	TF	500	0.00743	–
	CL-ITF-P	4 523	**0.00019**	80.61%
	CL-ITF-D	7 267	0.00027	72.24%
	STF	4 796	0.00065	33.67%
Hyper-Rössler (0.14)	FR	6 461	0.00599	–
	TF	2 788	<u>0.00435</u>	–
	CL-ITF-P	2 802	0.00366	15.86%
	CL-ITF-D	3 317	0.00326	25.06%
	STF	2 645	**0.00321**	26.21%
Lorenz (0.905)	FR	9 18	0.01209	–
	TF	4 67	<u>0.00152</u>	–
	CL-ITF-P	1 137	**0.00060**	60.53%
	CL-ITF-D	5 78	0.00135	11.18%
	STF	1 853	0.00511	−236.18%
Lorenz'96 (1.67)	FR	8 125	0.07273	–
	TF	4 175	<u>0.03805</u>	–
	CL-ITF-P	3 886	0.01680	55.85%
	CL-ITF-D	3 379	**0.01628**	57.21%
	STF	1 478	0.09030	−137.32%

The results (cp. Tab. V) show that STF provides improved performance compared to the best baseline for three of six datasets ranging from 26.21 – 46.75% relative improvement. For this it does require no additional hyperparameters if the systems LLE is known. It also beats the best performing CL strategy on the Hyper-Rössler dataset by a margin of 1.15%. For the rest of the datasets, the results stay behind those of the CL-ITF-x strategies showing a worse, i.e., increased, NRMSE by 7.00 – 236.18%. We assume

that where STF systematically induces TF to catch chaos preventing exploding gradients before they appear using knowledge about the processed data, CL helps the model to find more consistent minima in general not taking the degree of chaos into account. Originally, STF was not proposed to work for the kind of sequence-2-sequence architecture we are using, which may limit its effectiveness here. We further hypothesize that the GRU is in many cases able to keep the risk of exploding gradients low due to its gating mechanism and thus prevents STF to really show its full strength here.

For further investigation on CL for non-chaotic systems and to enrich our experiments, we conduct additional experiments that include the application of the baseline strategies TF and FR together with CL-ITF-P and CL-ITF-D on a periodic system and a measured real-world dataset. We use CL-ITF-P and CL-ITF-D since they provide the most consistent relative improvements in the essential experiments. As periodic system, we study the Thomas attractor (Thomas, 1999) with parameter $b = 0.32899$ which ensures a periodic behavior. Extending our evaluation to empirical data, we selected a time series used in the Santa Fe Institute competition (Weigend & Gershenfeld, 1993)[2].

Table VI: Comparing baseline strategies and CL-ITF-P on periodic Thomas and measured Santa Fe laser dataset

	Strategy	**Ł**	**Epochs**	**NRMSE ↓**	**Rel. impr. ↑**
Per. Thomas	FR	–	542	<u>0.00057</u>	–
	TF	–	542	0.00107	–
	CL-ITF-P	8 000	794	**0.00033**	42.11%
	CL-ITF-D	125	326	0.00045	21.05%
Santa Fe ($m = 20$)	FR	–	500	<u>0.02170</u>	–
	TF	–	22	0.04793	–
	CL-ITF-P	32 000	469	**0.02042**	5.90%
	CL-ITF-D	4 000	536	0.02232	−2.86%
Santa Fe ($m = 200$)	FR	–	208	<u>0.2786</u>	–
	TF	–	1	0.7104	–
	CL-ITF-P	64 000	1506	**0.2054**	26.27%
	CL-ITF-D	32 000	201	0.2950	−5.89%

The results in Table VI support our assumption that CL-ITF-x strategies are also successfully applicable for time series data originating dynamical systems with periodic behavior achieving relative improvements of 21.05 – 42.11%. Regarding the Santa Fe dataset we observe less impact by our strategies. Only having an improvement by 5.90% for CL-ITF-P and a worsening by 2.86% for CL-ITF-D on the empirical real-world data. When increasing the prediction horizon from 20 to 200 steps, we observe an increased relative improvement of 26.27% for CL-ITF-P. At the same time, we observe a relative decrease of −5.89% for CL-ITF-D. To investigate the radical difference between these results, we study the ϵ in relation to the appearance of TF steps in the respective training curriculum. Figure 10 shows two different probabilities along the training epochs. There is the TF probability ϵ that is directly determined by the curriculum function and $p_{\leq 200}$ which denotes the probability of a training sample to contain at least one TF step. It is computed as $p_{\leq 200} = \epsilon \sum_{i=1}^{200} (1-\epsilon)^{i-1}$ for the probabilistic strategy. For CL-ITF-D this probability is either 0 or 1 meaning that it only has an effect on training epochs ≥ 160. If we would use the same Ł as for CL-ITF-P here, the training would converge after 208 epochs just as in the plain FR case. CL-ITF-P though, due to its probabilistic nature, can sporadically induce TF steps for some of the batches in the earlier phase of training and thus provides a much smoother transition towards TF phase. We argue that this smoothness is crucial for the given task, which appears to be very sensitive to TF training steps.

We also conducted experiments for other RNN architectures, i.e., we selected a vanilla RNN, an LSTM, an unitary evolution RNN (uRNN) (Arjovsky et al., 2016) and a Lipschitz RNN (LRNN) (Erichson et al., 2020), in the same encoder-decoder setup as applied for the previous experiments with the GRU architecture. In

[2]https://github.com/tailhq/DynaML/blob/master/data/santafelaser.csv

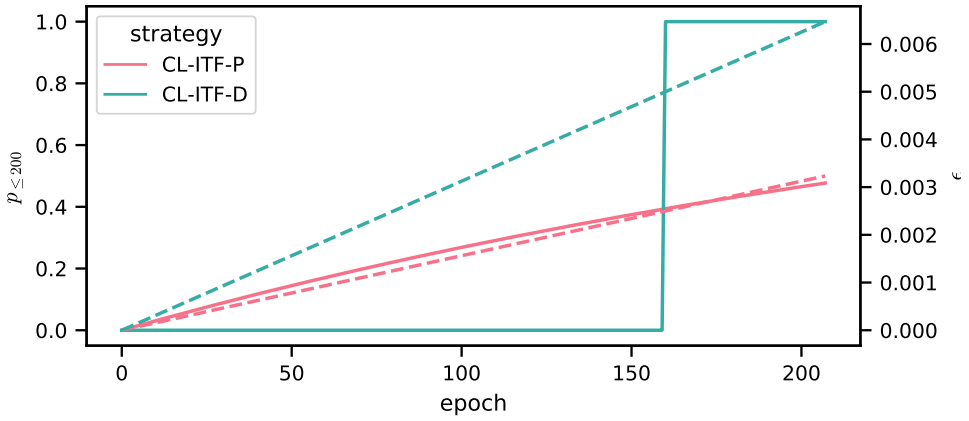

Figure 10: The probability course of a sample to include at least one TF step (solid) and the corresponding TF probability ϵ (dashed). Exemplary shown for the Santa Fe setup with 200 output steps (cp. Tab. VI).

the Table VII, we compare the NRMSE and relative improvement of these architectures on the four chaotic datasets from the exploratory experiments (cp. Tab. III). We compare TF, FR and previously best performing training strategies CL-ITF-P and CL-ITF-D (cp. Tab. IV). Except for one case, we observe that both CL strategies outperform the respective best performing baseline strategy on the vanilla RNN as well as the LSTM architecture. The only exception is a vanilla RNN trained to forecast the Lorenz'96 system using CL-ITF-P. This setup suffers a performance decrease by 83.45% while the NRMSE in all other experiments improves by 37.83 – 75.28% RNN and 26.04 – 69.75% LSTM respectively when using the CL strategies. The uRNN and the LRNN do not adapt their weight matrices directly while training but rather update several structured building block matrices to construct the actual weight matrices. We observe improvements from 0.4 to 77.75% and from 0.21 to 83.74% for the two architectures respectively. We provide more detailed information about these experiments can be found in appendix C.

In our experiments on the Lorenz'96 data, the performance of the encoder-decoder RNN remains an outlier. Especially, when we consider that for the deterministic variant CL-ITF-D there is a clear NRMSE improvement by 75.28%. We use this setup to take a closer look on the training gradients and process. In Figure 11a, we plot the mean of the decoder RNN gradient norm ($||\nabla W_d||$) over the training epochs for the CL-ITF-P and the CL-ITF-D case. We also add the teacher forcing probability ϵ and the learning rate η to the plot. For comparison with the two successful setups, we also give an overview of the gradient norm of the GRU and the LSTM based model under the same conditions (cp. Figs 11c and 11b).

For all models, we observe an oscillation of the gradient norm during CL-ITF-P training. CL-ITF-D avoids this behavior with a constant iteration scale curriculum that keeps the TF-FR-pattern fix for several epochs between the changes. The crucial epochs are indicated by green dashed vertical lines. In contrast, CL-ITF-P provides a probabilistic iteration scale curriculum that leads to intra epoch changes. The resulting variation in the gradient norm only stops when the training scale curriculum hits the final $\epsilon = 1$. Preceding that, the oscillating gradient norm originates from an unsteady training loss. Most of the time the unsteady loss can be compensated due to the increasing amount of TF over the epochs. For the Lorenz'96 data, however, it seems the unsteady loss together with the used scheduler leads to a rapid decrease of the learning rate. This effect is observable during the curriculum training of the basic RNN, the LSTM and the GRU. The latter two models seem to handle the resulting minimal learning rate of $3e^{-6}$ much better and manage to continue their training successfully.

To get an impression of the RNN's behavior without the unwanted learning rate drop we conducted the same CL-ITF-P experiments again without applying any learning rate scheduler. This time we plot the training loss, that exhibits the same oscillating behavior as the gradient norm, together with the validation loss, to see

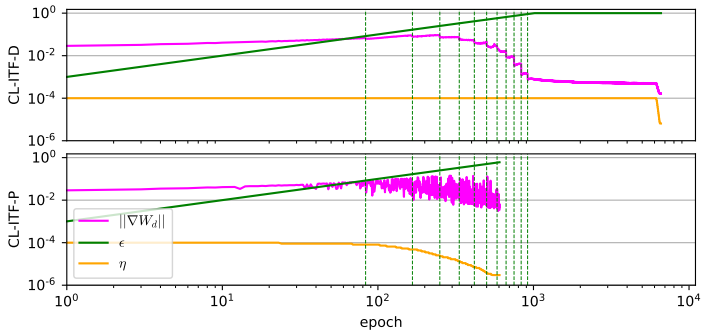

(a) RNN

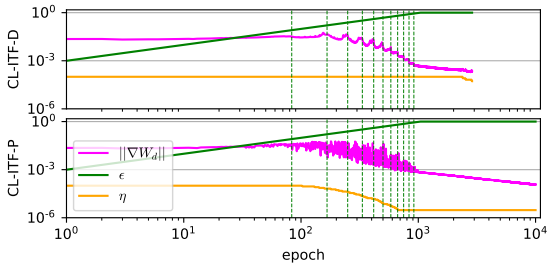

(b) LSTM

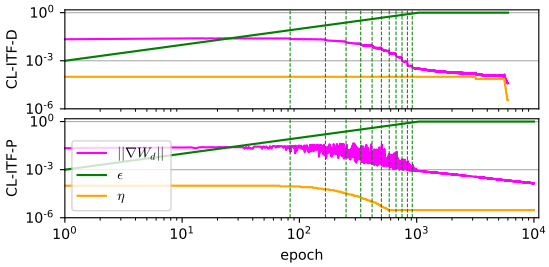

(c) GRU

Figure 11: Course of the average decoder gradient norm $||\nabla W_d||$ during training on Lorenz'96 data together with teacher forcing probability ϵ and learning rate η.

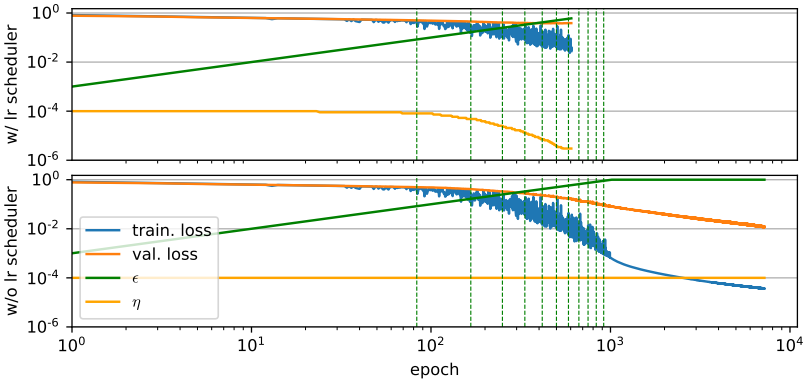

Figure 12: Course of the training and validation loss for the RNN on Lorenz'96 data using CL-ITF-P with and without learning rate scheduler.

if the change leads to improved loss values. The plot in Figure 12 shows that without the unwanted learning rate drop the basic RNN remains stable the transient phase towards $\epsilon = 1$ and ends up with a validation loss of 0.012 instead of 0.373. For the more sophisticated RNNs, we see clearly improved validation losses after much less epochs as well. The corresponding plots are shown in appendix B.

Table VII: Forecasting performance of additional RNNs (vanilla RNN, LSTM, unitary evolution RNN (uRNN) and Lipschitz RNN (LRNN)) on the different chaotic datasets. Given is the NRMSE with relative improvement in parenthesis for the CL strategies.

System	Strategy	RNN	LSTM	uRNN	LRNN
Thomas	FR	0.48117	0.43698	0.74991	0.11697
	TF	0.41274	0.05265	0.85679	0.05714
	CL-ITF-P	**0.17955** (56.50%)	0.01892 (64.06%)	**0.61889** (17.47%)	0.05237 (8.35%)
	CL-ITF-D	0.25659 (37.83%)	**0.01181** (77.57%)	0.73331 (2.21%)	**0.03926** (31.29%)
Rössler	FR	0.00747	0.00210	0.03726	0.27122
	TF	0.50174	0.00139	0.03317	0.90844
	CL-ITF-P	**0.00283** (62.12%)	**0.00063** (54.68%)	0.02473 (25.44%)	0.05185 (80.88%)
	CL-ITF-D	0.00319 (57.30%)	0.00085 (38.85%)	**0.02420** (27.04%)	**0.04409** (83.74%)
Lorenz	FR	0.11389	0.06526	0.13021	0.06675
	TF	0.00913	0.00169	0.96357	0.02830
	CL-ITF-P	0.00603 (33.95%)	**0.00075** (55.62%)	**0.03098** (76.21%)	**0.01732** (38.80%)
	CL-ITF-D	**0.00378** (58.60%)	0.00125 (26.04%)	0.02897 (77.75%)	0.02417 (14.59%)
Lorenz'96	FR	0.31002	0.13010	0.26359	0.62710
	TF	0.57870	0.22757	0.61159	0.65122
	CL-ITF-P	0.56872 (−83.45%)	**0.03935** (69.75%)	0.26253 (0.4%)	**0.62170** (0.86%)
	CL-ITF-D	**0.07663** (75.28%)	0.06855 (47.31%)	**0.18483** (29.88%)	0.62581 (0.21%)

6 Discussion

Baseline teaching strategies (RQ1). Considering the baseline teaching strategies FR and TF, we observe that per dataset one of the strategies performs substantially better than the other. We also observe that for the upper, based on their LLE, less chaotic datasets in Table IV FR performs better, while for the lower more chaotic datasets TF yields the better performing model. However, a larger study with more datasets would be required to justify this claim. Our takeaway is that none of the methods can universally recommended again motivating curriculum learning strategies.

Curriculum learning strategies (RQ2). Among the curriculum learning strategies, we observe that blending FR with a constant ratio of TF, i.e., CL-CTF-P, almost consistently yields worse results than the best performing baseline strategy and we therefore consider the strategy not relevant. The decreasing curricula CL-DTF-x that start the training with a high degree of teacher forcing and then incrementally reduce it to pure FR training partly perform better than the CL-CTF-P strategy and for a few datasets even

substantially better than the baseline. We also proposed and studied increasing curricula CL-ITF-x that start the training with no or a low degree of TF, which is then incrementally increased over the course of the training. We observe that these strategies consistently outperform not only the baseline strategies but all other tested curriculum learning strategies as well. However, it was not foreseeable when this would be the case making their application not suitable for new datasets without a lot of experimentation and tuning.

Training length (RQ3). Choosing an improper teaching strategy can result in an early convergence on a high level of generalization error, e.g., TF strategy for Mackey-Glass, Thomas, and Rössler. Models that yield better performance typically train for more iterations (cp. Tab. III and IV). However, a longer training may not necessarily yield a better performance, e.g., FR vs. TF for Lorenz. When considering the best performing CL-ITF-x strategies compared to the best performing baseline strategy, we observe moderately increased training iterations for some datasets, i.e., Thomas, Rössler, Hyper Rössler, Lorenz, but also decreased training iterations for other datasets, i.e., Mackey Glass and Lorenz'96. To better understand whether the longer training is the true reason for the better performing CL-ITF-x models, we compared their performance when only trained for as many iterations as the baseline model and still observe superior performance over the baseline model. In conclusion, we observe that the CL-ITF-x strategies facilitate a robust training reaching a better generalizing model in a comparable training time on all six tested datasets.

Prediction stability (RQ4). We evaluated the generalization as NRMSE for all models trained with the different training strategies per dataset while forecasting a dataset-specific horizon of 1 LT. However, this metric reflects only an average. When we strive for higher model performance on a multi-step prediction task we often aim for a longer prediction horizon at an acceptable error. To compare prediction stability, we report the NRMSE metric separately solely computed on the last 10% of the 1 LT horizon and additionally, we computed how many LTs per datasets can be predicted before falling below an R^2 of 0.9. We found that the CL-ITF-x strategies yielded the lowest NRMSE of the last 10% predicted values across all datasets and even more promising that these strategies facilitated the longest prediction horizon without falling below $R^2 = 0.9$. We conclude that the CL-ITF-x strategies may help models finding more stable minima in training, substantially improving their long-term forecasting performance.

Curriculum parametrization (RQ5). Initially, we evaluated curriculum learning strategies with a variety of different transition functions and individual start and end teacher forcing rate (cp. *exploratory* experiments). In these experiments, we observed high prediction performance of the CL-ITF-x strategies but with a diverse dataset-specific best performing curriculum meaning that the application of these strategies for new datasets would have necessitated an extensive hyper-parameter search. In a second set of *essential* experiments, we therefore explored whether we could identify curricula with less parametrization and a similar performance. We found those by using a linear transition that is solely configured by a single parameter Ł that determines the pace with which the teacher forcing increases or decreases over the course of the training. We found that these curricula were not only comparable to the previous transition functions and their parametrization but performed better for all four datasets that we evaluated in both experimental sets and yielded the best performing model across all six datasets in the second experiment.

Iteration scale curriculum (RQ6). Having the CL-ITF-x strategies outperforming the CL-DTF-x strategies leads to rethinking the hitherto common intuition of supporting the early phases of training by TF and moving towards FR in the later stages of training. Rather, we hypothesize that this lures the model into regions of only seemingly valid and stable minima in which they stay even during the more FR heavy epochs resulting in a premature termination of the training. This hypothesis is supported by the resulting loss curves for the respective experiments. For example, for the increasing curriculum case, a look at the training duration and the course of the ϵ (c.p., Fig. 8) shows that a training that starts off with FR can enable the model to train much longer in the pure TF zone later. This is compared to the case where solely TF is used. The difference between the two CL-ITF-x strategies is how the prescribed amount of teacher forcing is distributed across the prediction steps of one training iteration (aka epoch). While the CL-ITF-D strategy distributes them as one cohesive sequence, the CL-ITF-P strategy distributes them randomly across the training sequence. We found that in the *essential* experiments with the linear transition the CL-ITF-P strategy performed overall best for four of the six datasets and would have also be a good choice with a substantial gain over the best performing baseline training strategy for the other two datasets. In conclusion, we observe that the CL-ITF-P strategy trains models that yield 16–81% higher performance than a

conventional training with FR or TF. Apart from that, the *essential* results do not lead to a clear conclusion whether to use CL-ITF-P or CL-ITF-D in a given case. The above-mentioned most obvious difference in the distribution of TF steps firstly may lead to a more coherent backpropagation in the deterministic variant, but it also results in a different behavior regarding maximum number of consecutive FR steps (TF-gap) for a given ϵ. Having the same curriculum function applied for CL-ITF-P and CL-ITF-D, therefore makes the TF-gap decrease much faster in the early training stage for the probabilistic variant. Further, it changes the TF-gap in a logarithmic rather than a linear fashion as for CL-ITF-D. This difference cannot be compensated by parametrizing the curriculum length demonstrating the need for the two strategies. Plus, this only affects the mean TF-gap produced by CL-ITF-P, which has a variance of $\frac{1-\epsilon}{\epsilon^2}$ due to its geometric distribution. Therefore the TF-gap also varies a lot in the early training stage. In the context of the result Tables VI and VII, we see the probabilistic and the deterministic type of CL-ITF-x can exhibit disfunctions in some specific cases. More thorough investigation of such cases is required to further improve CL strategies, make them more generally applicable and fully identify their limitations.

Limitations of this work. Our observations allow us to draw conclusions regarding appropriate curricula for the training of sequence-to-sequence RNN on continuous time series data. Where in our study, the data originates from dynamical systems that predominantly impose chaotic behavior. Consequently, all observations made here are currently limited to this kind of models and data. We acknowledge that more research is necessary to clarify several uncertain points. First, regarding the question why an increasing curriculum tends to find more stable minima throughout all studied datasets. Leading to the question, what determines a proper curriculum and parametrization. A first step could be to shift the focus on the baseline strategies again to extract primary conditions under which trainings get unstable. Therefore, a closer look at the weights and behavior of the model gradients during training, the statistics of the gradient of the processed time series and the used sampling rate is required at least. Finally, a more thorough investigation on empirical real-world data improving on the early and inconclusive results on the Santa Fe dataset (cp. Tab. VI) is needed to reveal the capabilities and limitations of different CL strategies in this regard.

Application in other domains. In this paper we focus exclusively on the field of time series forecasting. In principle the proposed strategies could easily be applied to ML models exhibiting autoregressive predictions trained for other domains. For example, sequence-to-sequence RNNs and transformers for Automatic Machine Translation (AMT). As mentioned before, scheduled sampling, that is included in the CL-DTF-x strategies, was originally proposed, and successfully used to improve the training of RNNs for NLP but, on the other hand, performed rather poorly for time series forecasting in our experiments. Thus, we cannot draw any conclusions about the usefulness of CL-ITF-x strategies in other domains based on our results either. Therefore, evaluating the effectiveness of increasing curricula in other domains remains a task for future work at this point and would go beyond the focus of our study.

7 Conclusions

While training encoder-decoder RNNs to forecast time series data, strategies like teacher forcing produce a discrepancy between training and inference mode, i.e., the exposure bias. Curriculum learning strategies like scheduled sampling or training directly in free running mode are used to reduce this effect. We run an extensive series of experiments using six chaotic dynamical systems as benchmark and observed that not for all of them the exposure bias yields a crucial problem. We see that even an FR training that is per definition free of the exposure bias effect may not be optimal. In fact we observed for one half of our datasets TF performs better and for the other half FR. With the focus on curriculum learning strategies like scheduled sampling, we proposed two novel strategies and found that those yield models that consistently outperform the best performing baseline model by a wide margin of 15–80% NRMSE in a multi-step prediction scenario over one Lyapunov time. We found that these models are robust in their prediction allowing to forecast longer horizons with a higher performance. We found it sufficient to parametrize the strategy with a single additional parameter adopting the pace of the curriculum.

References

Martin Arjovsky, Amar Shah, and Yoshua Bengio. Unitary evolution recurrent neural networks. In *International conference on machine learning*, pp. 1120–1128. PMLR, 2016.

Samy Bengio, Oriol Vinyals, Navdeep Jaitly, and Noam Shazeer. Scheduled sampling for sequence prediction with recurrent neural networks. In *Advances in Neural Information Processing Systems*, pp. 1171–1179, 2015.

Julien Brajard, Alberto Carrassi, Marc Bocquet, and Laurent Bertino. Combining data assimilation and machine learning to emulate a dynamical model from sparse and noisy observations: A case study with the lorenz 96 model. *Journal of Computational Science*, 44:101171, 2020.

Reggie Brown, Paul Bryant, and Henry DI Abarbanel. Computing the lyapunov spectrum of a dynamical system from an observed time series. *Physical Review A*, 43(6):2787, 1991.

Tom B Brown, Benjamin Mann, Nick Ryder, Melanie Subbiah, Jared Kaplan, Prafulla Dhariwal, Arvind Neelakantan, Pranav Shyam, Girish Sastry, Amanda Askell, et al. Language models are few-shot learners. *arXiv preprint arXiv:2005.14165*, 2020.

Kathleen Champion, Bethany Lusch, J Nathan Kutz, and Steven L Brunton. Data-driven discovery of coordinates and governing equations. *Proceedings of the National Academy of Sciences*, 116(45):22445–22451, 2019.

Bo Chang, Minmin Chen, Eldad Haber, and Ed H Chi. Antisymmetricrnn: A dynamical system view on recurrent neural networks. *arXiv preprint arXiv:1902.09689*, 2019.

Kyunghyun Cho, Bart Van Merriënboer, Dzmitry Bahdanau, and Yoshua Bengio. On the properties of neural machine translation: Encoder-decoder approaches. *arXiv preprint arXiv:1409.1259*, 2014.

Junyoung Chung, Caglar Gulcehre, KyungHyun Cho, and Y. Bengio. Empirical evaluation of gated recurrent neural networks on sequence modeling. *arXiv preprint arXiv:1412.3555*, 12 2014.

Jacob Devlin, Ming-Wei Chang, Kenton Lee, and Kristina Toutanova. Bert: Pre-training of deep bidirectional transformers for language understanding. *arXiv preprint arXiv:1810.04805*, 2018.

Jonathan B Dingwell. Lyapunov exponents. *Wiley encyclopedia of biomedical engineering*, 2006.

Qingyun Dou, Yiting Lu, Joshua Efiong, and Mark JF Gales. Attention forcing for sequence-to-sequence model training. *arXiv preprint arXiv:1909.12289*, 2019.

Konstantinos Drossos, Shayan Gharib, Paul Magron, and Tuomas Virtanen. Language modelling for sound event detection with teacher forcing and scheduled sampling. *arXiv preprint arXiv:1907.08506*, 2019.

N Benjamin Erichson, Omri Azencot, Alejandro Queiruga, Liam Hodgkinson, and Michael W Mahoney. Lipschitz recurrent neural networks. *arXiv preprint arXiv:2006.12070*, 2020.

William Gilpin. Chaos as an interpretable benchmark for forecasting and data-driven modelling. *arXiv preprint arXiv:2110.05266*, 2021.

Ian Goodfellow, Jean Pouget-Abadie, Mehdi Mirza, Bing Xu, David Warde-Farley, Sherjil Ozair, Aaron Courville, and Yoshua Bengio. Generative adversarial nets. *Advances in neural information processing systems*, 27:2672–2680, 2014.

Ian Goodfellow, Yoshua Bengio, and Aaron Courville. *Deep learning*. MIT press, 2016.

Haohan Guo, Frank K Soong, Lei He, and Lei Xie. A new gan-based end-to-end tts training algorithm. *arXiv preprint arXiv:1904.04775*, 2019.

Michael D Hartl. Lyapunov exponents in constrained and unconstrained ordinary differential equations. *arXiv preprint physics/0303077*, 2003.

Tianxing He, Jingzhao Zhang, Zhiming Zhou, and James Glass. Quantifying exposure bias for neural language generation. *arXiv preprint arXiv:1905.10617*, 2019.

Sepp Hochreiter and Jürgen Schmidhuber. Long short-term memory. *Neural computation*, 9(8):1735–1780, 1997.

Anil Kag and Venkatesh Saligrama. Time adaptive recurrent neural network. In *Proceedings of the IEEE/CVF Conference on Computer Vision and Pattern Recognition*, pp. 15149–15158, 2021.

Anil Kag, Ziming Zhang, and Venkatesh Saligrama. Rnns incrementally evolving on an equilibrium manifold: A panacea for vanishing and exploding gradients? In *International Conference on Learning Representations*, 2019.

DP Kingma, LJ Ba, et al. Adam: A method for stochastic optimization. 2015.

Georgia Koppe, Hazem Toutounji, Peter Kirsch, Stefanie Lis, and Daniel Durstewitz. Identifying nonlinear dynamical systems via generative recurrent neural networks with applications to fmri. *PLoS computational biology*, 15(8):e1007263, 2019.

Alex M Lamb, Anirudh Goyal Alias Parth Goyal, Ying Zhang, Saizheng Zhang, Aaron C Courville, and Yoshua Bengio. Professor forcing: A new algorithm for training recurrent networks. In *Advances in neural information processing systems*, pp. 4601–4609, 2016.

Zongyi Li, Nikola Kovachki, Kamyar Azizzadenesheli, Burigede Liu, Kaushik Bhattacharya, Andrew Stuart, and Anima Anandkumar. Fourier neural operator for parametric partial differential equations. *arXiv preprint arXiv:2010.08895*, 2020.

Zongyi Li, Nikola Kovachki, Kamyar Azizzadenesheli, Burigede Liu, Kaushik Bhattacharya, Andrew Stuart, and Anima Anandkumar. Markov neural operators for learning chaotic systems. *arXiv preprint arXiv:2106.06898*, 2021.

Rui Liu, Berrak Sisman, Jingdong Li, Feilong Bao, Guanglai Gao, and Haizhou Li. Teacher-student training for robust tacotron-based tts. In *ICASSP 2020-2020 IEEE International Conference on Acoustics, Speech and Signal Processing (ICASSP)*, pp. 6274–6278. IEEE, 2020.

Edward N Lorenz. Deterministic nonperiodic flow. *Journal of the atmospheric sciences*, 20(2):130–141, 1963.

Edward N Lorenz. Predictability: A problem partly solved. In *Proc. Seminar on predictability*, volume 1, 1996.

Bethany Lusch, J Nathan Kutz, and Steven L Brunton. Deep learning for universal linear embeddings of nonlinear dynamics. *Nature communications*, 9(1):1–10, 2018.

Michael C Mackey and Leon Glass. Oscillation and chaos in physiological control systems. *Science*, 197 (4300):287–289, 1977.

Chenfeng Miao, Shuang Liang, Minchuan Chen, Jun Ma, Shaojun Wang, and Jing Xiao. Flow-tts: A non-autoregressive network for text to speech based on flow. In *ICASSP 2020-2020 IEEE International Conference on Acoustics, Speech and Signal Processing (ICASSP)*, pp. 7209–7213. IEEE, 2020.

Tsvetomila Mihaylova and André FT Martins. Scheduled sampling for transformers. *arXiv preprint arXiv:1906.07651*, 2019.

Zahra Monfared, Jonas M Mikhaeil, and Daniel Durstewitz. How to train rnns on chaotic data? *arXiv preprint arXiv:2110.07238*, 2021.

Garrett Nicolai and Miikka Silfverberg. Noise isn't always negative: Countering exposure bias in sequence-to-sequence inflection models. In *Proceedings of the 28th International Conference on Computational Linguistics*, pp. 2837–2846, 2020.

Jakub Nowak, Ahmet Taspinar, and Rafał Scherer. Lstm recurrent neural networks for short text and sentiment classification. In *International Conference on Artificial Intelligence and Soft Computing*, pp. 553–562. Springer, 2017.

Kishore Papineni, Salim Roukos, Todd Ward, and Wei-Jing Zhu. Bleu: a method for automatic evaluation of machine translation. In *Proceedings of the 40th annual meeting of the Association for Computational Linguistics*, pp. 311–318, 2002.

Jaideep Pathak, Zhixin Lu, Brian R Hunt, Michelle Girvan, and Edward Ott. Using machine learning to replicate chaotic attractors and calculate lyapunov exponents from data. *Chaos: An Interdisciplinary Journal of Nonlinear Science*, 27(12):121102, 2017.

Alec Radford, Jeffrey Wu, Rewon Child, David Luan, Dario Amodei, Ilya Sutskever, et al. Language models are unsupervised multitask learners. *OpenAI blog*, 1(8):9, 2019.

Krishnan Radhakrishnan and Alan C Hindmarsh. Description and use of lsode, the livermore solver for ordinary differential equations. 1993.

Marc'Aurelio Ranzato, Sumit Chopra, Michael Auli, and Wojciech Zaremba. Sequence level training with recurrent neural networks. *arXiv preprint arXiv:1511.06732*, 2015.

OE5889510996 Rossler. An equation for hyperchaos. *Physics Letters A*, 71(2-3):155–157, 1979.

Otto E Rössler. An equation for continuous chaos. *Physics Letters A*, 57(5):397–398, 1976.

T Konstantin Rusch and Siddhartha Mishra. Coupled oscillatory recurrent neural network (cornn): An accurate and (gradient) stable architecture for learning long time dependencies. *arXiv preprint arXiv:2010.00951*, 2020.

T Konstantin Rusch, Siddhartha Mishra, N Benjamin Erichson, and Michael W Mahoney. Long expressive memory for sequence modeling. *arXiv preprint arXiv:2110.04744*, 2021.

Marco Sandri. Numerical calculation of lyapunov exponents. *Mathematica Journal*, 6(3):78–84, 1996.

Matteo Sangiorgio and Fabio Dercole. Robustness of lstm neural networks for multi-step forecasting of chaotic time series. *Chaos, Solitons & Fractals*, 139:110045, 2020.

Masaki Sano and Yasuji Sawada. Measurement of the lyapunov spectrum from a chaotic time series. *Physical review letters*, 55(10):1082, 1985.

Dominik Schmidt, Georgia Koppe, Zahra Monfared, Max Beutelspacher, and Daniel Durstewitz. Identifying nonlinear dynamical systems with multiple time scales and long-range dependencies. *arXiv preprint arXiv:1910.03471*, 2019.

Florian Schmidt. Generalization in generation: A closer look at exposure bias. *arXiv preprint arXiv:1910.00292*, 2019.

Ljubisa Sehovac and Katarina Grolinger. Deep learning for load forecasting: Sequence to sequence recurrent neural networks with attention. *IEEE Access*, 8:36411–36426, 2020.

Ljubisa Sehovac, Cornelius Nesen, and Katarina Grolinger. Forecasting building energy consumption with deep learning: A sequence to sequence approach. In *2019 IEEE International Congress on Internet of Things (ICIOT)*, pp. 108–116. IEEE, 2019.

Lawrence F Shampine and Skip Thompson. Solving ddes in matlab. *Applied Numerical Mathematics*, 37(4): 441–458, 2001.

Guorui Shen, Jürgen Kurths, and Ye Yuan. Sequence-to-sequence prediction of spatiotemporal systems. *Chaos: An Interdisciplinary Journal of Nonlinear Science*, 30(2):023102, 2020.

Julien Clinton Sprott and Konstantinos E Chlouverakis. Labyrinth chaos. *International Journal of Bifurcation and Chaos*, 17(06):2097–2108, 2007.

Rohan Thavarajah, Xiang Zhai, Zheren Ma, and David Castineira. Fast modeling and understanding fluid dynamics systems with encoder–decoder networks. *Machine Learning: Science and Technology*, 2(2): 025022, 2021.

René Thomas. Deterministic chaos seen in terms of feedback circuits: Analysis, synthesis," labyrinth chaos". *International Journal of Bifurcation and Chaos*, 9(10):1889–1905, 1999.

Pantelis R Vlachas, Wonmin Byeon, Zhong Y Wan, Themistoklis P Sapsis, and Petros Koumoutsakos. Data-driven forecasting of high-dimensional chaotic systems with long short-term memory networks. *Proceedings of the Royal Society A: Mathematical, Physical and Engineering Sciences*, 474(2213):20170844, 2018.

Rui Wang, Eugenia Kalnay, and Balakumar Balachandran. Neural machine-based forecasting of chaotic dynamics. *Nonlinear Dynamics*, 98(4):2903–2917, 2019.

Andreas S Weigend and Neil A Gershenfeld. Results of the time series prediction competition at the santa fe institute. In *IEEE international conference on neural networks*, pp. 1786–1793. IEEE, 1993.

Ronald J Williams and David Zipser. A learning algorithm for continually running fully recurrent neural networks. *Neural computation*, 1(2):270–280, 1989.

Zhilin Yang, Zihang Dai, Yiming Yang, Jaime Carbonell, Russ R Salakhutdinov, and Quoc V Le. Xlnet: Generalized autoregressive pretraining for language understanding. *Advances in neural information processing systems*, 32, 2019.

Wenpeng Yin, Katharina Kann, Mo Yu, and Hinrich Schütze. Comparative study of cnn and rnn for natural language processing. *arXiv preprint arXiv:1702.01923*, 2017.

A Training and Validation Loss Curves

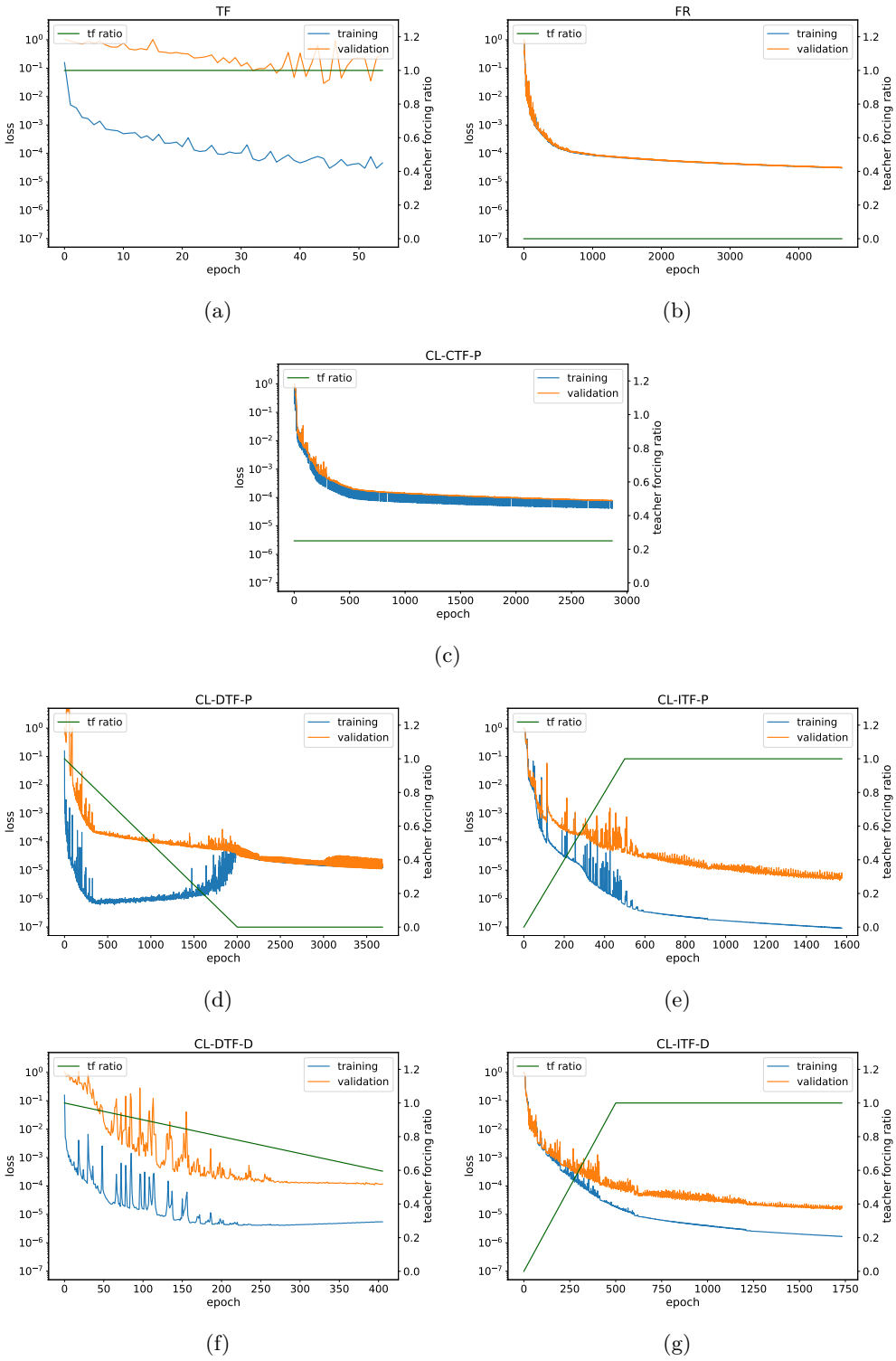

Figure 13: Training and validation loss for Mackey-Glass

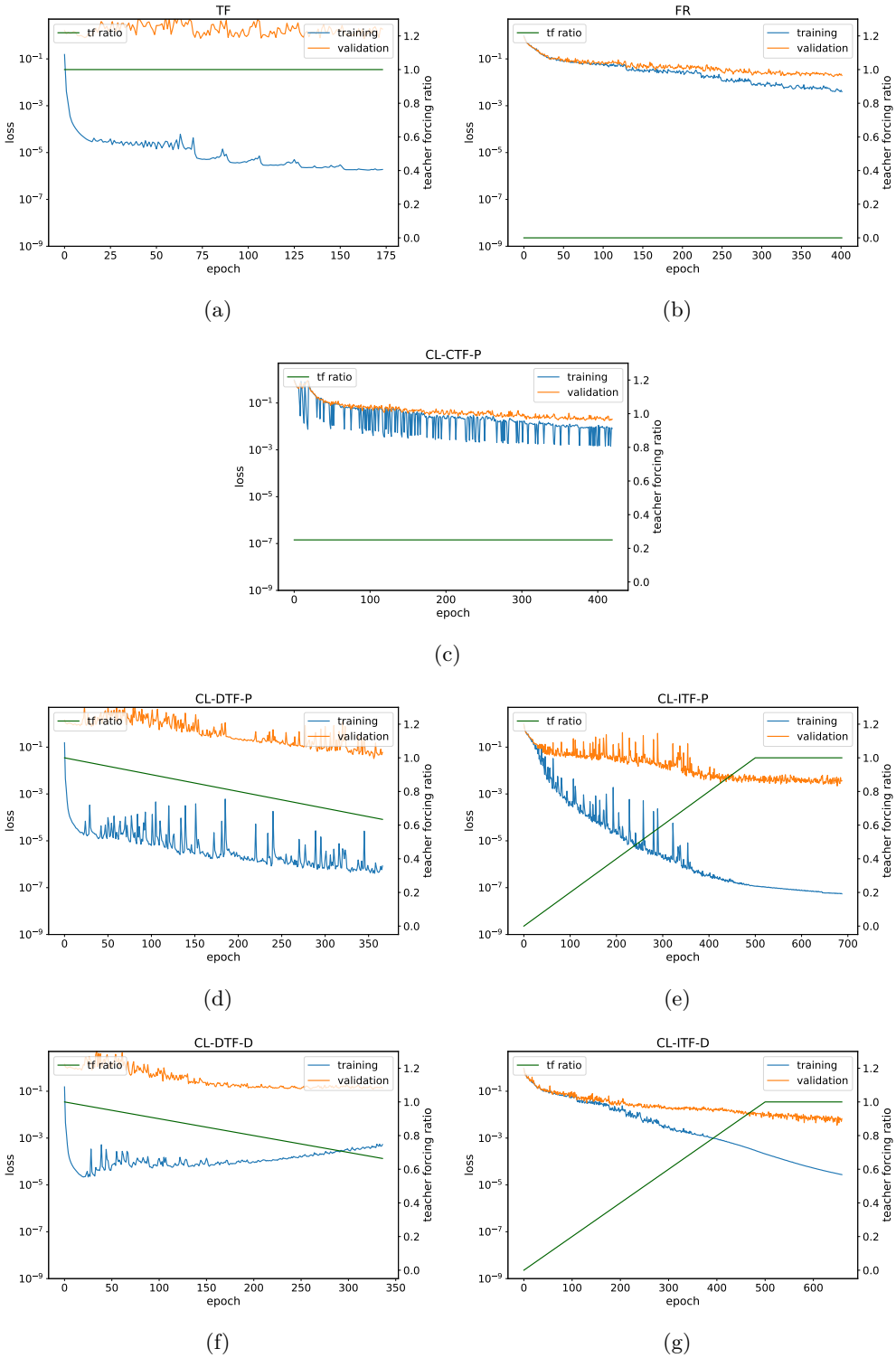

Figure 14: Training and validation loss for Thomas

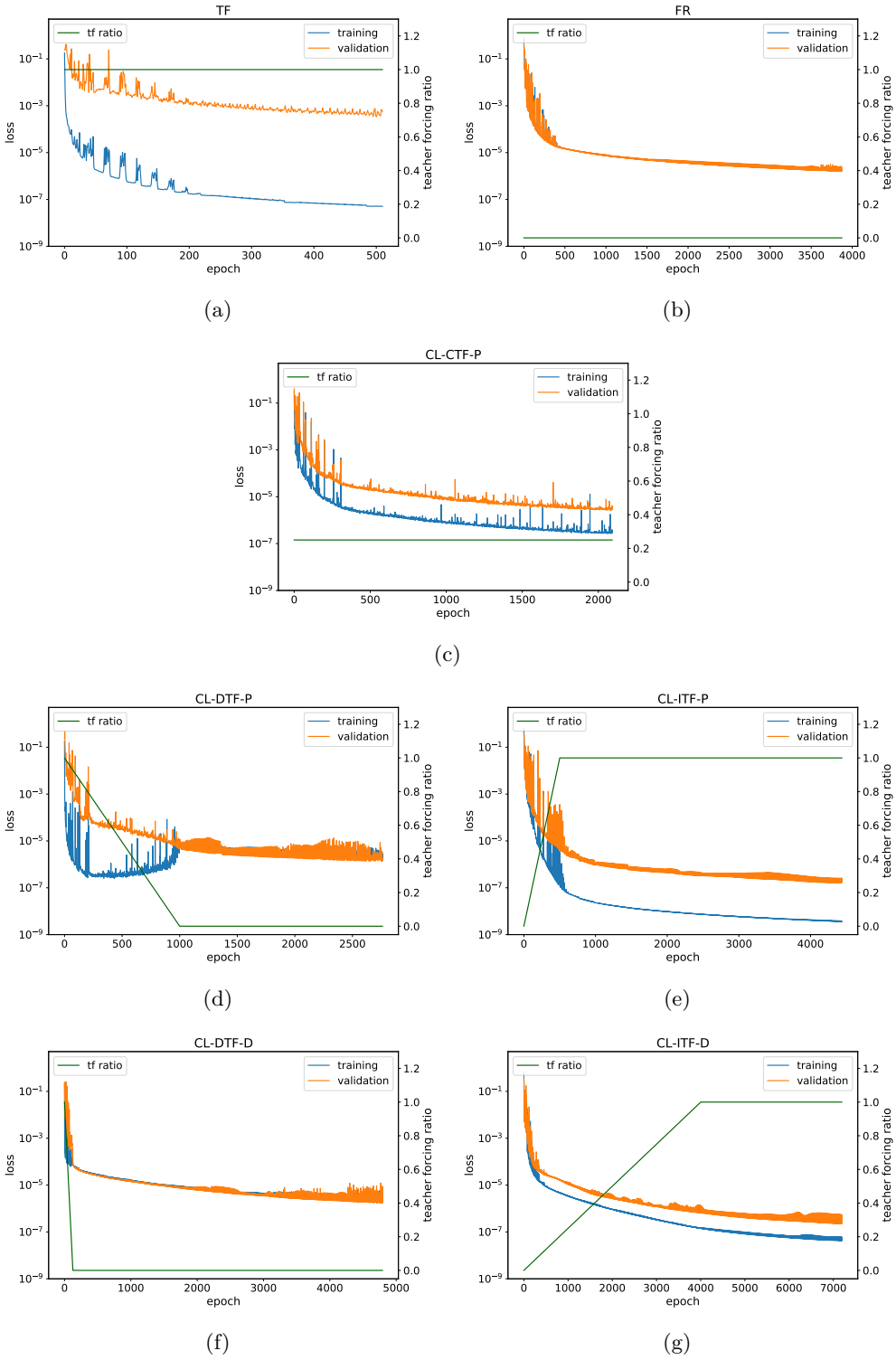

Figure 15: Training and validation loss for Rössler

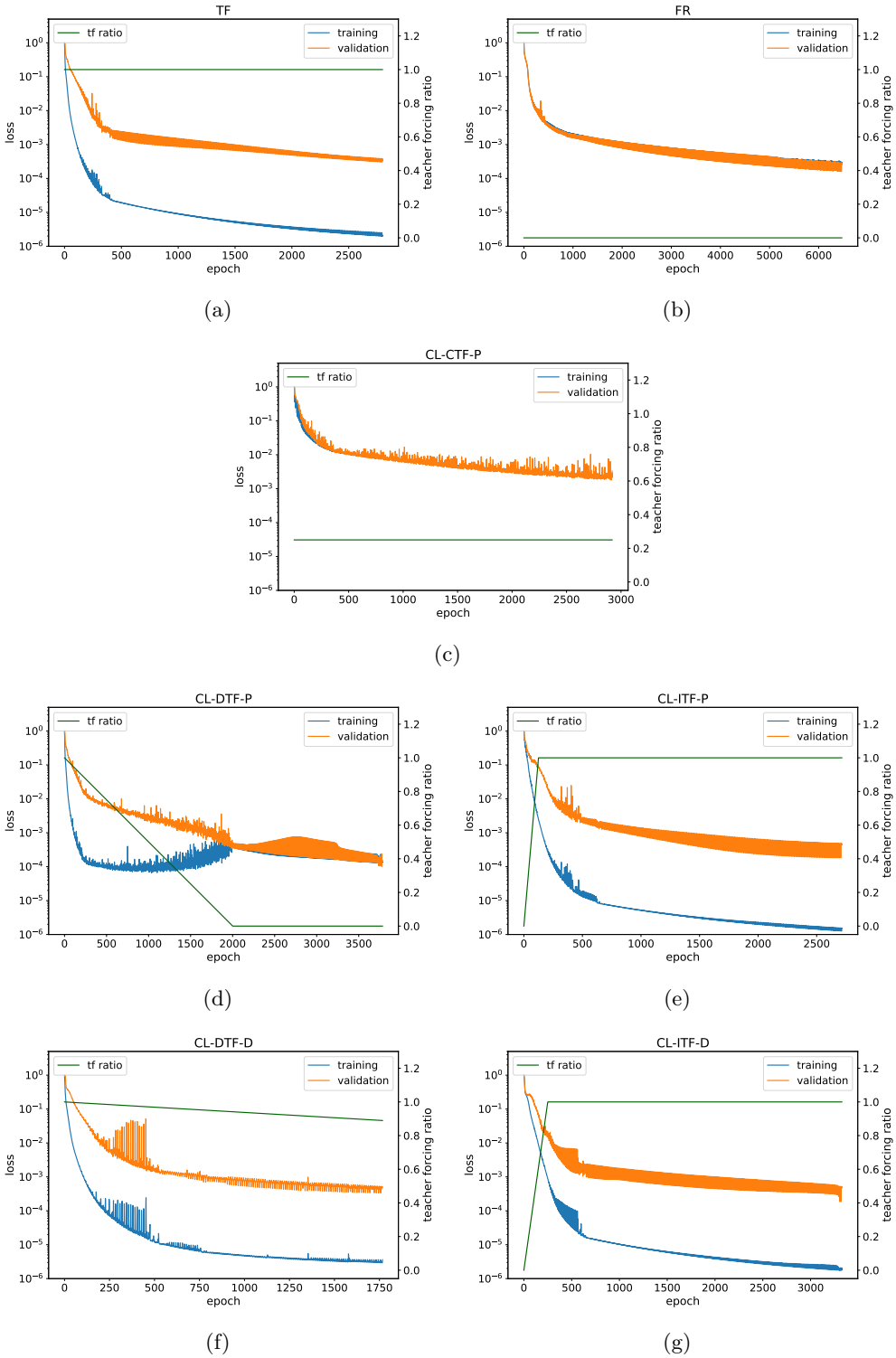

Figure 16: Training and validation loss for Hyper-Rössler

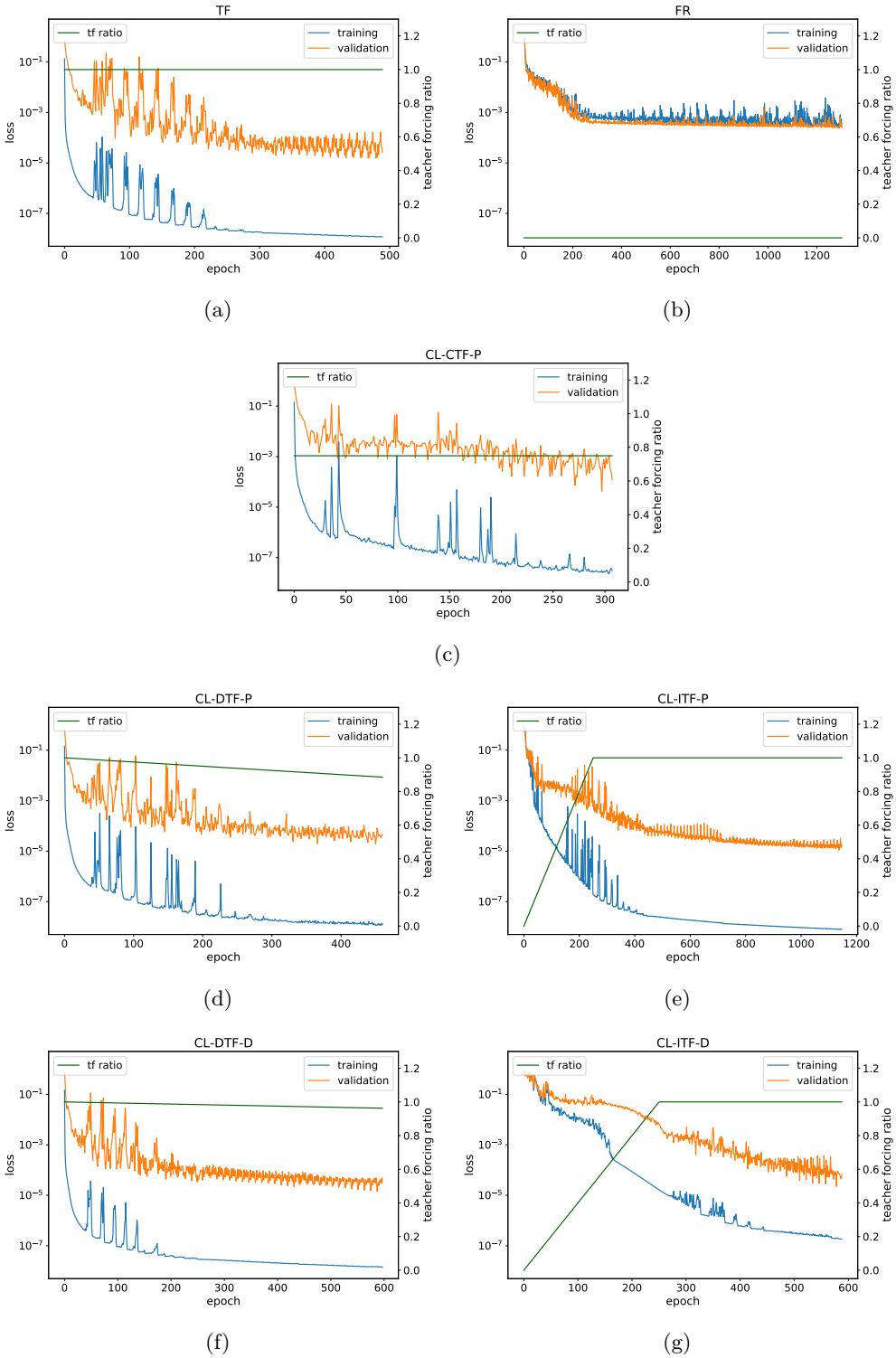

Figure 17: Training and validation loss for Lorenz

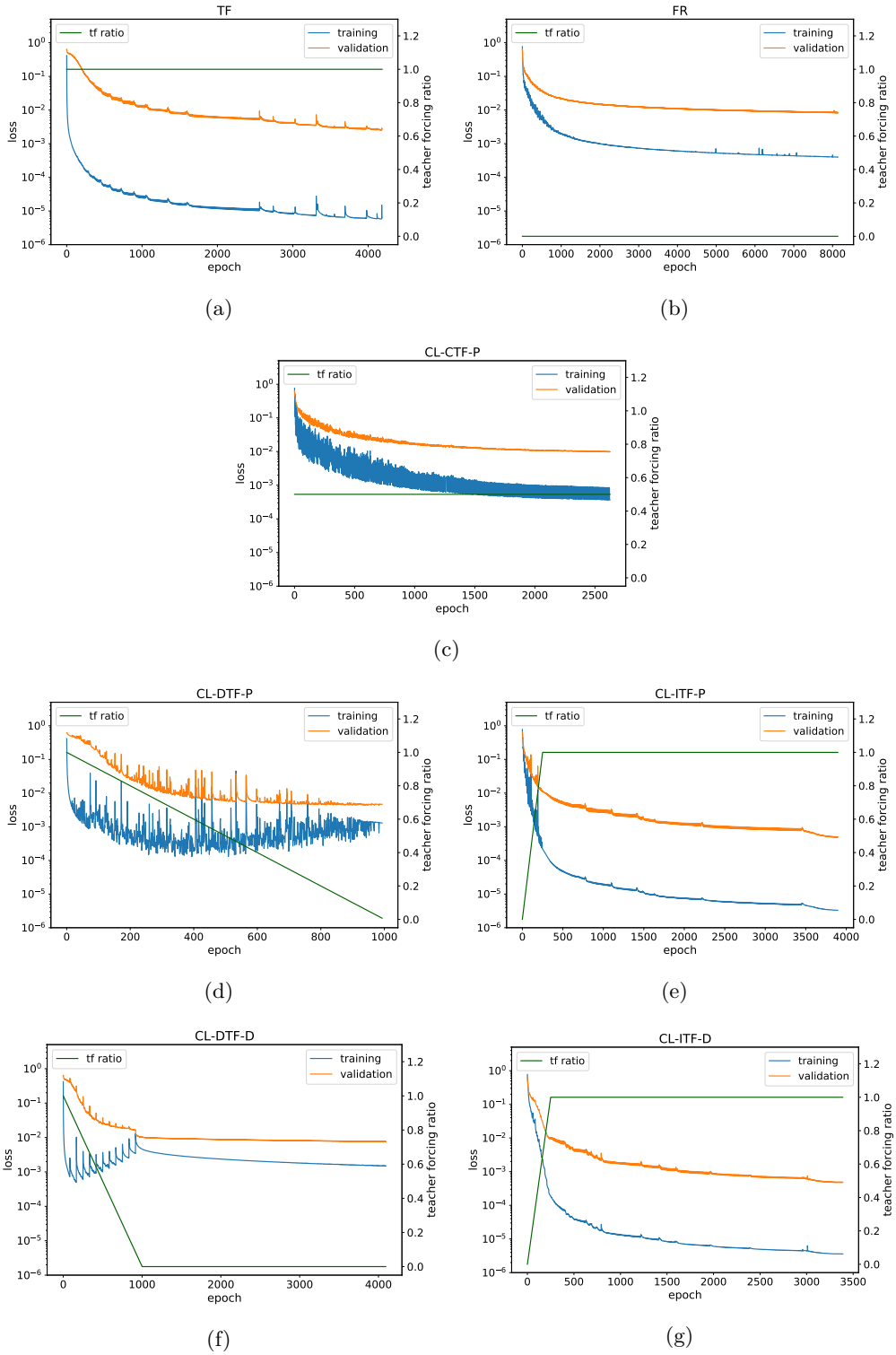

Figure 18: Training and validation loss for Lorenz'96

B CL-ITF-P With and Without LR Scheduler

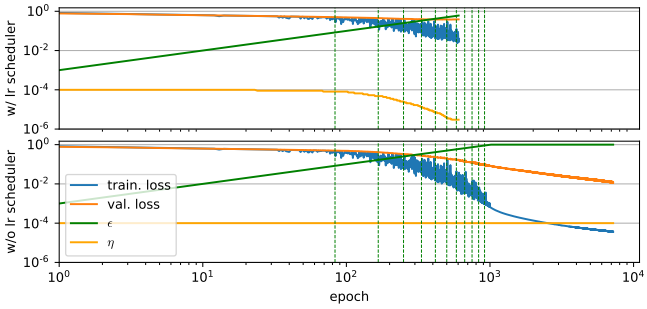

(a)

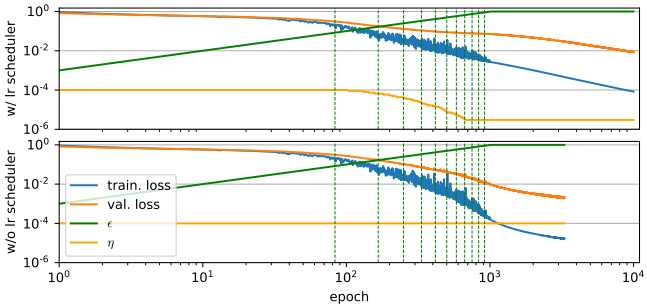

(b)

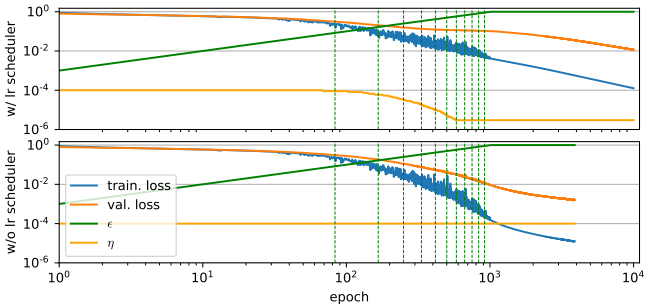

(c)

Figure 19: Course of the training and validation loss for the basic RNN (a), LSTM (b) and GRU (c) on Lorenz'96 data with and without using a learning rate scheduler.

C Different RNN Models

Table VIII: Forecasting performance of the vanilla RNN on four different chaotic datasets

System	Strategy	Ł	Epochs	NRMSE ↓	Rel. impr. ↑
Thomas	FR	–	51	0.48117	–
	TF	–	249	0.41274	–
	CL-ITF-P	1 000	266	**0.17955**	56.50%
	CL-ITF-D	250	183	0.25659	37.83%
Rössler	FR	–	2 292	0.00747	–
	TF	–	1	0.50174	–
	CL-ITF-P	500	2 063	**0.00283**	62.12%
	CL-ITF-D	1 000	3 075	0.00319	57.30%
Lorenz	FR	–	506	0.11389	–
	TF	–	572	0.00913	–
	CL-ITF-P	1 000	746	0.00603	33.95%
	CL-ITF-D	125	782	**0.00378**	58.60%
Lorenz'96	FR	–	1 710	0.31002	–
	TF	–	637	0.57870	–
	CL-ITF-P	1 000	505	0.56872	−83.45%
	CL-ITF-D	1 000	6 573	**0.07663**	75.28%

Table IX: Forecasting performance of the LSTM on four different chaotic datasets.

System	Strategy	Ł	Epochs	NRMSE ↓	Rel. impr. ↑
Thomas	FR	–	45	0.43698	–
	TF	–	818	0.05265	–
	CL-ITF-P	250	758	0.01892	64.06%
	CL-ITF-D	125	859	**0.01181**	77.57%
Rössler	FR	–	2 417	0.00210	–
	TF	–	1 650	0.00139	–
	CL-ITF-P	1 000	3 426	**0.00063**	54.68%
	CL-ITF-D	250	2 367	0.00085	38.85%
Lorenz	FR	–	1 154	0.06526	–
	TF	–	398	0.00169	–
	CL-ITF-P	250	806	**0.00075**	55.62%
	CL-ITF-D	31	419	0.00125	26.04%
Lorenz'96	FR	–	4 019	0.13010	–
	TF	–	3 721	0.22757	–
	CL-ITF-P	500	9 164	**0.03935**	69.75%
	CL-ITF-D	62	4 509	0.06855	47.31%

Table X: Forecasting performance of the unitary evolution RNN on four different chaotic datasets.

System	Strategy	Ł	Epochs	NRMSE ↓	Rel. impr. ↑
Thomas	FR	–	354	0.74991	–
	TF	–	53	0.85679	–
	CL-ITF-P	64 000	359	**0.61889**	17.47%
	CL-ITF-D	64 000	340	0.73331	2.21%
Rössler	FR	–	911	0.03726	–
	TF	–	1 287	0.03317	–
	CL-ITF-P	1 000	1 126	0.02473	25.44%
	CL-ITF-D	500	1 402	**0.02420**	27.04%
Lorenz	FR	–	758	0.13021	–
	TF	–	4	0.96357	–
	CL-ITF-P	1 000	758	**0.03098**	76.21%
	CL-ITF-D	500	1 096	0.02897	77.75%
Lorenz'96	FR	–	1 043	0.26359	–
	TF	–	398	0.61159	–
	CL-ITF-P	2 000	697	0.26253	0.4%
	CL-ITF-D	2 000	1 335	**0.18483**	29.88%

Table XI: Forecasting performance of the Lipschitz RNN on four different chaotic datasets.

System	Strategy	Ł	Epochs	NRMSE ↓	Rel. impr. ↑
Thomas	FR	–	879	0.11697	–
	TF	–	928	0.05714	–
	CL-ITF-P	250	879	0.05237	8.35%
	CL-ITF-D	500	1 191	**0.03926**	31.29%
Rössler	FR	–	3 704	0.27122	–
	TF	–	79	0.90844	–
	CL-ITF-P	250	2 304	0.05185	80.88%
	CL-ITF-D	500	3 149	**0.04409**	83.74%
Lorenz	FR	–	1 298	0.06675	–
	TF	–	625	0.02830	–
	CL-ITF-P	62	914	**0.01732**	38.80%
	CL-ITF-D	250	686	0.02417	14.59%
Lorenz'96	FR	–	489	0.62710	–
	TF	–	469	0.65122	–
	CL-ITF-P	1 000	477	**0.62170**	0.86%
	CL-ITF-D	4 000	489	0.62581	0.21%